UiT The Arctic University of Norway

Chrysochromulina leadbeateri

- *Understanding the Presumed Causal Agent Behind the Harmful Algal Bloom of 2019*

Erlend Grann-Meyer

BIO-3955 *Master's thesis in Akvamedisin,* August 2020

Faculty of Biosciences, Fisheries and Economics

Norwegian College of Fishery Science

Acknowledgements

Til Astrid,

In hindsight, my short-lived dedication to the scientific endeavor was extreme. I neglected the things that really matter in life.

Though I am grateful for everyone helping me out throughout what I consider the ‘worst year of my life’ – nothing compares to the comfort you provided me when I needed it the most.

Jeg er evig takknemlig – tusen hjertelig takk

UiT, Norwegian College of Fishery Science

Trondheim, December 2022

Erlend Grann-Meyer

Hans Christopher Bernstein

Abstract

In the Spring of 2019, a harmful algal bloom (HAB) of *Chrysochromulina leadbeateri* decimated 14 500 tonnes of caged salmon in the Northern Norwegian coastal regions. *C. leadbeateri* is a natural part of the marine microbiome along the Norwegian coast, and similar events have happened in the past. To heighten our understanding of how these HABs develops, and capacity of the causal agent as a harmful species, we've assessed the environmental and enumeration data of *C. leadbeateri* density in Northern Troms, collected by Akvaplan Niva during the 2019 HAB, in concurrence with the assessment of several microbial isolation and genomic extraction techniques.

The highest cell counts of *C. leadbeateri* existed in *Balsfjorden*, where, at most, an estimated ∼49 million cells/L resided at 3 m below the surface. Further, we found a temporal correspondence between an increase in *C. leadbeateri* cell counts and increased salmon mortality at a locality in Kattfjorden. Generally, there was a higher density of *C. leadbeateri* at 3, compared with 10 m. This discrepancy could plausibly be attributed to divergent water densities between the two measurement depths. The algal isolation and genomic extraction attempts proved largely unsuccessful. Thus, we provide a series of corrections to the techniques used, to ensure that future attempts may be more efficacious.

Keywords – *Chrysochromulina leadbeateri*, 2019, Harmful algal bloom, Northern Norway, Aquaculture

Contents

List of Figures

List of Tables

1 Introduction

In May 2019, the first reports of increased salmon mortality were received from Ofotfjorden - soon confirmed to be algae-related. Similar reports were promptly received from the adjacent Astafjorden. Followed by Vestfjorden and Tysfjorden - until the final reports of mortality were disseminated from fish farms on the western side of Kvaløya. Several water samples, with high cell counts of *C. leadbeateri*-like haptophyta, were concurrently taken throughout the Troms region. Curiously, without the associated mortality. By the end of June, the bloom had subsided.

During this harmful algal bloom (HAB), salmon farmers sent the M2 Research Group a large volume of water samples. UiT also launched a rapid response monitoring program, which, in part, included sampling of frozen fish gills from afflicted areas, in concord with the targeted cultivation of *C. leadbeateri* - the suspected causal agent.

1.1 Main objectives

Besides the HAB occuring in the spring of 2019, the northern coastal regions of Norway have experienced similar events related to *C. leadbeateri* - especially in 1991 - but also smaller events, in 1998 and 2008. Since the last, 'great' HAB of 1991, the toolbox of science has expanded, notably in the field of genomics. Hence, this most recent event has been the only known opportunity to apply modern, genome-enabled molecular tools, and then to use them to understand which taxa correspond with which environmental factors during these devastating HABs.

The original goal of this thesis, was to further explain the HAB's toxicity, interspecies relations, as well as fully sequencing *C. leadbeateri*'s genome, with long-read sequencing methods, to gain deeper insight into its functional capacity as a harmful species - which proved to be a lot harder than expected. As the project progressed, Akvaplan-Niva, a private research company, gave us access to a large volume of data pertaining to the 2019 HAB. Thus, the main objectives of this thesis is twofold: showcasing the inaugural analysis of the environmental and taxonomical data collected by Akvaplan-Niva in the Northern Troms-region; and, presenting the preliminary results from the methods developed to extract and isolate algal deoxyribonucleic acid (DNA).

1.2 2019 HAB - collaboration and sampling

The 2019 HAB covered a large geographic area, and high cell counts of *C. leadbeateri* was not necessarily tied to increased mortality in near-by fish farms. As such, there were few indications regarding which localities would be hit next - consequently supplying us with the necessary samples.

Initial contact was established with several seafood companies throughout Northern Norway - some already supplying us with water samples from at-risk locations - resulting in them giving us permission to gather gill samples, should they experience any mortality. The term 'at-risk' locations, throughout this thesis, is used to denote the fish farms which, at the time, were not necessarily afflicted by *C. leadbeateri*-induced mortality, but were imperilled, due to their geographic proximity to the HAB.

If any outbreak were to happen in the vicinity of Tromsø, we were capable of responding, though, we were restrained by time, resources, and personnel to cover a larger area - and we reached out for help. The response, in almost all cases, were extremely supportive, and several private fish health companies were on stand-by to collect afflicted gill samples - in case of further blooming.

We obtained fish gill samples for microbial genomic DNA (gDNA)-extraction from 4 geographically distinct fish farms (Figure 3.1). Each experiencing varying degrees of fish mortality. Attempts at isolating *C. leadbeateri*-like Haptophyta (Figure 4.9), was performed on enriched water samples, collected at 3 different fish farms in the Troms-region (Figure 3.2). From the fish farms supplying us with samples, we also received corresponding mortality figures - collected in accordance with regulation June 17th 2008 nr. 822 'akvakulturdriftsforskriften'.

Attempts at CTAB gDNA-extraction was performed on UIO-035, a strain of *C. leadbeateri* isolated during the HAB of 1991. The data collected by Akvaplan-Niva, was analyzed, on the condition that no individual fish farms would be identified. Hence, all the localities they sampled, at, or near fish farms, are given names, based on the fjord they were situated in, supplied with latitude and longitude coordinates (WGS 84). This policy was extended to all the fish farms sampled throughout this thesis.

2 Background

2.1 Harmful algal blooms

Blooms of phytoplankton, with related fish mortality and other 'nuisances', have been reported throughout history. By some believed to be an act of god, the accounts given in Exodus 7:14-25 of "*the water was changed into blood*" and "*the fish in the Nile died, and the river smelled so bad that the Egyptians could not drink its water*", could arguably be one of the earliest recorded events.

Commonly, and often erroneously, called 'red tides', harmful algal blooms (HABs) affect virtually every coastal region of the world (Anderson, 2009). In scientific writing, the latter term is preferred. 'HAB', excludes many blooms which might discolour the water, without any associated 'nuisances', and also includes blooms of highly toxic cells, of varying colouration. The term also includes blooms, who, even at low concentrations, may create nuisances, without any associated discolouration (Anderson et al., 2012). According to Paerl (1988), a HAB differs from other algal blooms by certain universally translated 'nuisances'. He allocates these nuisances into three categories: **1)** perceivable water quality deterioration, including trophic changes; **2)** chronic or intermittent health hazards - to humans and other organisms, via toxins or increased microbial growth (Watson, 2013); and **3)** losses of aesthetic, and hence recreational values of afflicted waters.

Before a HAB develops, cells might be present at low concentrations, often persisting in the background for months (Anderson et al., 2012). Elseways, the HAB will be initiated elsewhere, being delivered to an adjacent region via advection (Raine et al., 2010). Further aspects of the HAB-phenomena, might also be explained by resting cysts, where the germination provides the inoculom for blooms, and the decline is initiated when vegetative cells are transformed back into a resting stage (Anderson et al., 2005; Garces et al., 2010).

The geographic distribution of phytoplankton is substantially controlled by sea-surface temperatures (SST (Anderson et al., 2012; Thomas et al., 2012)). Often, the realized niche of a HAB, is defined within a narrow range of SSTs (Hattenrath et al., 2010; Moore et al., 2008). Through ocean global warming (Levitus et al., 2009) and changing distributions of temperature niches (Robson et al., 2016), it's likewise expected that the range and

distribution of phytoplankton and HABs will shift (Hallegraeff, 2010). Climate-change driven warming of the oceans can be unevenly distributed (Baumann and Doherty, 2013), notably along the coast lines (Wu et al., 2012). Modelling by Gobler et al. (2017), seems to demonstrate that ocean warming in the North Atlantic, increased both the potential growth rate and bloom season for several toxic algae. In addition to nutrient discharges from agri- and aquaculture (Davidson et al., 2014), and increased monitoring (Hallegraeff, 2010) - the apparent increase in HABs worldwide, might also be a consequence of increased climate variability (Moore et al., 2008; Gobler et al., 2017).

Scientific and technological development, concurrent with the expansion and heightened importance of aquaculture, has resulted in increased detection and identification of harmful algae (Maso and Garcés, 2006). Moreover, the increased exploitation of coastal resources, also brought forth an exponential growth in accompanying monitoring programs, further accumulating the reports of toxic events and other nuisances (Hallegraeff, 1993, 2010).

HABs might cause acute mortalities of both wild and farmed fish (Bruslé, 1995). After establishing salmon farming on the Pacific coast in the 1970s, both Chile (Guzmán et al., 1975; Montes et al., 2018) and Canada (Black, 1990; Horner et al., 1997), would experience recurring HAB-induced fish mortality and nuisances (Montes et al., 2018; Haigh and Esenkulova, 2014). HABs have also afflicted salmon farming in New Zealand (Chang et al., 1990), and Scotland (Bruno et al., 1989).

From the microalgal species with important socio-economic impact, $\sim$ 100 have been identified as toxin-producing, of which 70% are dinoflagellates (Díaz et al., 2019; Moestrup, 2009). Besides producing toxins, which might damage the gills or digestive system of fish (ichthytoxins), HABs might also cause direct adverse effects, by irritating the gills - causing excess mucus production, leading to hypoxia and anoxia (Treasurer et al., 2003). In Norway, ichthyotoxic algae has mainly been represented by the haptophytes *C. leadbeateri* (unknown mechanism) (Rey et al., 1991; Rey, 1998), *Prymnesium polylepis* (previously *Chrysochromulina polylepis*) (Dahl et al., 1989), and *Prymnesium parvum* (Johnsen et al., 2010). Similar events, have also been caused by the dictyophyte *Pseudochattonella farcimen* (Jakobsen et al., 2012), and the dinoflagellates *Gyrodinium aureolum* (Dahl and Tangen, 1993) and *Alexandrium excavatum* (Tangen and Dahl, 1993).

2.2 *Chrysochromulina leadbeateri*

C. leadbeateri was first described by Estep et al. (1984), from materials collected in the eastern North Atlantic. It was described as "*chloroplast containing cells, 1.5-4.0 µm in diameter when dried*", "*with two slightly subequal flagella, ca. 11 µm and 13 µm long*", and with a "*haptonema longer than flagella, and in 8-18 coils*". They named the haptophyte in honour of B. S. C. Leadbeater, who earlier had described scales of a similar construction, collected from the Norwegian coast (Leadbeater, 1972), which together with scales collected in Australian waters by Hallegraeff (1983), were included in the circumscription of the species (Eikrem and Throndsen, 1998).

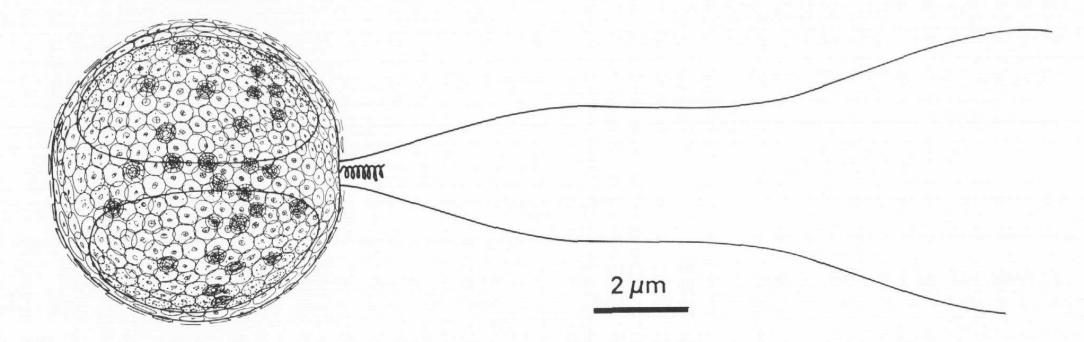

Figure 2.1: *Schematic drawing of UIO-035, based light and electron microscopy. The spherical cell measures 3-8 µm in diameter, with two flagella of slightly unequal length (13-16 and 16-20 µm), and a coiled haptonema. The appendages are inserted apically. The two large chloroplasts are parietal, and occupies a large part of the cell (Eikrem and Throndsen, 1998). Reprinted with permission from J. Throndsen.*

Eikrem and Throndsen (1998) gave the first description of in *vitro*, live material. They isolated the strain UIO-035, from the Lofoten area into unialgal cultures during the 1991 HAB. In contrast with the holotype (Estep et al., 1984), they only observed 4-8 coils in the haptonema, as well as noticeable differences in scale morphology. Since the original description, genome-enabled phylogenetic tools, based on nucleotide sequences in the small (18S rRNA) and large (28S rRNA) subunit ribosomal DNA (Medlin et al., 1997; Edvardsen et al., 2011), have radically changed the traditional taxonomic classification of several species belonging to the genus *Chrysochromulina* (Chrétiennot-Dinet et al., 2014). *C. leadbeateri* remains an outlier, being the only member of its genus without a saddle-shaped cell, and not having its flagella inserted subapically and ventrally (Edvardsen et al., 2011).

2.2.1 Earlier *C. leadbeateri*-induced HAB-events

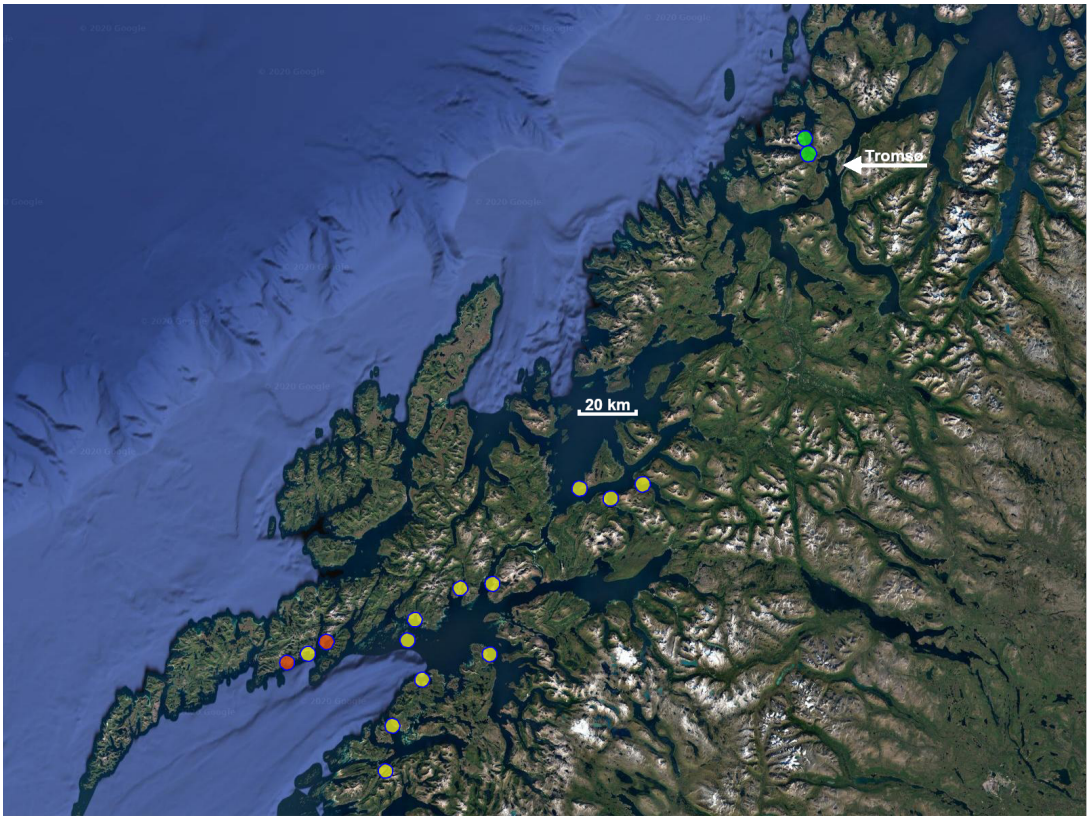

Figure 2.2: *Localities historically afflicted by HAB-induced mortality. Those afflicted by the HAB in 1991 are marked in yellow (Rey and Aure, 1991), 1998 in green (Appendix A1), and 2008 in orange (Berget, 2008b). Map template provided by SolarGIS web service (Šúri et al., 2011).*

The 1991 HAB, was first reported May 16th, when all the salmon on board a well boat - travelling from Lødingen to Skrova, across Vestfjorden - died (Rey et al., 1991). It would continue until June 20th, wasting between 420 (Rey et al., 1991) and 600 (Johnsen et al., 1999) tonnes of caged salmon. Peak mortality was experienced in the period May 24-28th, afflicting localities in Vestfjorden and adjacent fjords (marked with yellow in Figure 2.2). Noteworthy, compared to the HAB of *P. polylepis* in Skagerakk in 1988 (Dahl et al., 1989), mostly caged salmon were afflicted, with the wild fauna, apparently, managing to swim away (Johannessen et al., 1991).

Sampling throughout Troms and Finnmark revealed small concentrations of *C. leadbeateri*, before any advection from Vestfjorden could have inoculated these waters, contributing to the idea that *C. leadbeateri* is a natural part of the marine microbiome along the Norwegian coast (Hegseth and Eilertsen, 1991).

At the time, Rey et al. (1991) concluded that the most effective early warning system for HABs along the Norwegian coast, was the open pens of the salmon farmers. These pens, would, over the years, expand into new Northern-Norwegian fjords (Finansdepartementet, 2019) - indirectly and involuntarily, contributing reports of ichthyotoxicity in HABs which might otherwise have remained unnoticed (Hallegraeff, 1993).

May 1998, two fish farms, in Kaldfjorden (marked with green in Figure 2.2), reported HAB-induced mortality (Rey, 1998). Water samples showed large concentrations of *Chrysochromulina* sp., including *C. leadbeateri*, as well as two unidentified *Chrysochromulina*-like Haptophyta (Appendix A1).

May 2008, an aquarium in Lofoten, and a nearby fish farm (marked with orange in Figure 2.2), experienced moderate *C. leadbeateri*-induced mortality (Berget, 2008a). The reports of adverse effects, would last for a few weeks (Berget, 2008b).

2.2.2 The HAB of Spring 2019

In 1991, a regulatory change legalized the ownership of more than a single fish farm (Hovland, 2014). From 1991 to 2019, the aquaculture industry consolidated and industrialised (Hersoug, 2014), and the Norwegian biomass of cage-reared salmon, would increase nearly 9-fold (Finansdepartementet, 2019). Concurrently, the three northernmost counties, increased its relative share of this production, from 30 to 43 % (SSB, 1992; Berget, 2020). In 1991, there were no fish farms in the inner part of Ofotfjorden (Johannessen et al., 1991), in 2019, these would be the first to be afflicted (Karlsen et al., 2019).

From May 5th to June 7th, 2019, (Karlsen et al., 2019; Fiskeridirektoratet, 2019), 14 500 tonnes of salmon would perish, at the time, representing ∼2% of the total Norwegian biomass (Marthinussen et al., 2020). Still, HAB-induced deaths, only accounted for ∼ 14 percent of the total salmon 'wastage[1]' in 2019 (Veterinærinstituttet, 2020).

[1]The term 'wastage', is used to denote biomass lost to 'unnatural causes'. The natural cause being slaughter. Veterinærinstituttet recently stopped using the term, preferring to cite the actual number of salmon deaths (Veterinærinstituttet, 2019).

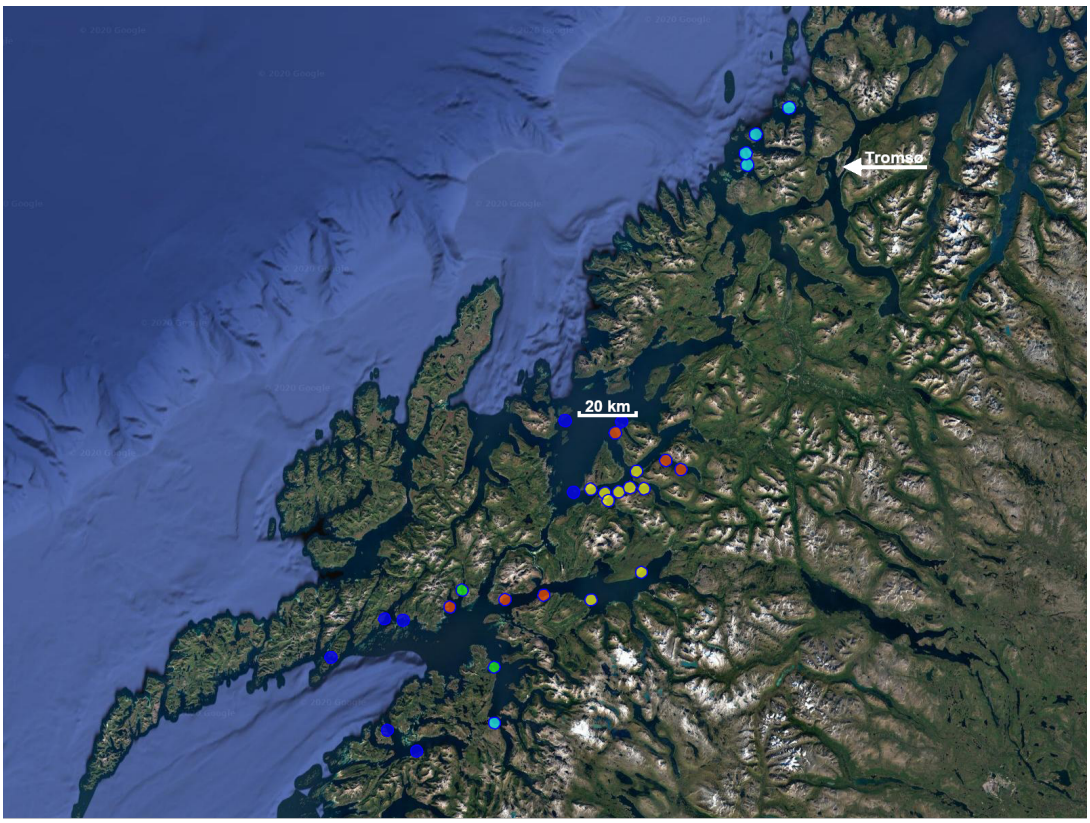

Figure 2.3: *Localities directly or indirectly afflicted by the 2019 HAB. The colour-scheme is based on the dates which Fiskeridirektoratet (2019) confirmed HAB-induced mortality, illustrated in the mapping-tool provided by ManolinAqua (2019). The localities confirmed as directly afflicted before May 17th, are marked in yellow; May 21-22 in orange; between May 25-30th in green; and June 5-7 in cyan. Indirectly afflicted localities - those which experienced a marked economic disruption by the HAB - are coloured in blue. Indirect effects include:* ***(1)*** *being stocked with sickly fish, by well boats traversing through HAB-afflicted areas;* ***(2)*** *having to expedite slaughter of smaller salmon;* ***(3)*** *moving the fish entirely, to an unaffected locality. All indirectly afflicted localities, were identified by cross-referencing maps from Marthinussen et al. (2020) with the BarentsWatch fish health web service (BarentsWatch, 2020). Not shown, are two localities in Finnmark, apparently afflicted by being stocked with sickly, HAB-afflicted salmon (Karlsen et al., 2019). Map template provided by SolarGIS web service (Šúri et al., 2011).*

May 5th, anomalous fish mortality were noticed at localities in Ofotfjorden [2], sporadically continuing until June 4th (Fiskeridirektoratet, 2019). May 11th, a locality at the outer edge of Ofotfjorden - between Tjeld- and Ramsundet - notified the Norwegian Food safety Authority, reporting anomalous fish mortality [3].

[2]Based on Karlsen et al. (2019) reporting that a fish farming company - who at the time, only had 3 active localities, all in Ofotfjorden (BarentsWatch, 2020) - experienced mortality.

[3]Karlsen et al. (2019) reports that a fish farming company, with only one locality in Ofotfjorden, made this notice. Of their two localities afflicted during the bloom (Fiskeridirektoratet, 2019), this one was immediately adjacent to already afflicted areas.

May 14th, salmon farming companies with localities in Astafjorden, reported acute fish mortality (Karlsen et al., 2019). May 16th, further localities in Astafjorden - including a location from which we later would collect gill samples (section 3.1.1.1) - would disseminate similar reports (Karlsen et al., 2019). 10 localities in Astafjorden would be directly afflicted by the HAB - none reporting acute mortality after May 17th (Fiskeridirektoratet, 2019).

May 19th, a warning was issued to the fish farmers in the outer edge of Ofotfjorden - based on current modelling and continuing mortality in the inner fjord - that the HAB would likely spread (Fiskeridirektoratet, 2019). May 20th, a locality at the outer edge of Ofotfjorden, which had already experienced anomalous fish mortality on May 11th, would again be afflicted[4]. May 22nd, a locality near Rinøya - in Vestfjorden, right next to Tjeldsundet - experienced acute fish mortality (Karlsen et al., 2019; Fiskeridirektoratet, 2019), followed on May 25th, by a neighbouring locality, further east, in Kanstadfjorden [5].

After May 22th, fish from several at-risk locations were moved to safer localities (Karlsen et al., 2019), reducing the effectiveness of using fish farms to monitor the further distribution of the HAB. At-risk locations also stopped feeding, which might have reduced the HAB's ichthyotoxic potential (Rensel and Whyte, 2003). One fish farmer - from which we also received mortality figures and water samples (section 3.1.2.2) - stopped feeding, continuously, for 3 weeks.

May 30th, a locality on the outer edge of Tysfjorden, would report acute mortality. When we later received mortality figures from this locality, we discovered an even larger HAB-event, occurring on May 18th (section 3.1.1.2).

June 4th, 4 localities on the western side of Kvaløya, reported HAB-induced mortality (Fiskeridirektoratet, 2019), including localities from which we gathered gill- (section 3.1.1.3), and water samples (section 3.1.2.2). June 7th, the last ichthyotoxic event would be recorded, when a salmon farmer experienced ∼75% mortality trying to stock up fish in the inner part of Tysfjorden (Fiskeridirektoratet, 2019).

[4]May 20th is the date Karlsen et al. (2019) reports that the fish farming company with the one locality in the outer edge of Ofotfjorden experienced acute mortality. Fiskeridirektoratet (2019) would confirm *C. leadbeateri*-induced mortality May 21st.

[5]By now, the testing capabilities and responsiveness of Fiskeridirektoratet (2019) had increased. Combined with Karlsen et al. (2019) being mostly concerned with when the different salmon farming companies were first afflicted, and their subsequent 'responsiveness' - the reports disseminated from Fiskeridirektoratet (2019), in the later part of the HAB, now, provides a comparably higher resolution of information.

2.2.3 Causes and mechanism

Rey et al. (1991) made an educated guess, that the 1991 HAB started in the Ofot-/Tysfjorden area, in the latter part of April. They could not ascertain if the HAB was then spread by advection from this area, or, if there was several HABs, all starting out in fjords with similar environmental conditions. Rey et al. (1991) deemed it most likely, that "*the bloom was triggered by a special combination of seasonal development of biological and physical environmental conditions and physiological characteristics of this type of algae*", and that "*the seasonal increase of freshwater runoff led to the spreading of harmful algae first to the Vestfjorden and thereafter, through the Tjeldsundet, northwards to the Astafjord area*".

Rey et al. (1991) further speculated, that the 1991 HAB could possibly have ended due to being washed out by spring flood, predation of zooplankton, or other environmental conditions (Heidal et al., 1991). After May 17th, 1991, the concentrations of *C. leadbeateri* rapidly decreased, and was soon supplanted by diatoms (Rey and Aure, 1991).

The winter of 1990/1991, continued a series of mild winters in Norway, making coastal waters warmer than normal (Rey and Aure, 1991). There was also an increased and earlier freshwater runoff in the winter/spring 1991, leading to lower salinities, and, possibly, an enhancement of the stratification in the water column, subsequently triggering an estuarine circulation, with outflow of brackish water to the inner part of Vestfjorden (Rey and Aure, 1991). This could result in the spring bloom starting earlier, and - combined with heavy cloudiness, increased winds and rainfall - developing slower. Rey et al. (1991) deemed it possible, that a period of fair weather at end of April - combined with the strengthened stratification and increased outflow of brackish water - could contribute to the initiation of the HAB and its subsequent spread.

In the winter of 2018/2019 - December through February - the drainage basin surrounding Ofotfjorden, would be 1.5-2 ^{o}C warmer than the normal temperature [6] (Grinde and Mamen, 2019b); in March, it would fall back to normal (Grinde and Mamen, 2019d); before rising to 2-3 ^{o}C above average in April (Grinde and Mamen, 2019a); falling back to normal in May (Grinde and Mamen, 2019c).

[6] The 'normal temperature' is the monthly average, measured from 1961 to 1991 (Grinde and Mamen, 2019b)

The same area, would concurrently experience an elevated precipitation - rising to 250-400 % of normal[7] in February (Grinde and Mamen, 2019b); 200-300% in March (Grinde and Mamen, 2019d); falling back to normal in April (Grinde and Mamen, 2019a); normal precipitation levels continuing till the end of May (Grinde and Mamen, 2019c).

In the immediate aftermath of the 2019 HAB, Landstad (2019) speculated that expansion hydro-power - after the 1980s, in the drainage basins surrounding Ofotfjorden - had "*shifted the seasons geophysical, hydro-chemical and biological processes*". She further speculated that the changed environmental conditions - with less estuarine circulation and increased stratification - could suppress the normal bloom of diatoms, making the area more susceptible to toxic blooms of *C. leadbeateri*. As shown in Figure 2.4, there's a high density of hydro-power plants, surrounding the suspected epicenter of both the 1991 and 2019 HAB.

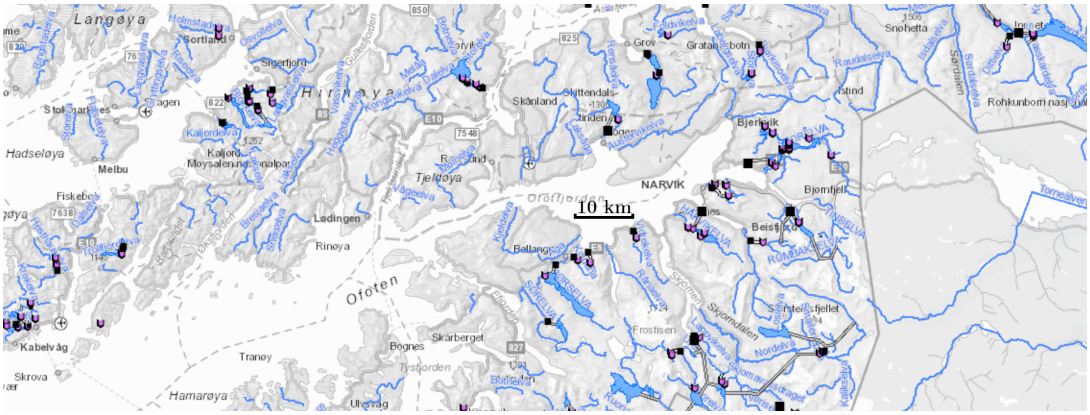

Figure 2.4: *Map illustrating hydro-power plants and rivers surrounding the Ofot-/Vest-/Astafjord-basins. Black squares represent hydro-power plants, purple 'shields' represent dams, and black bordered, gray lines represent water tunnels. Map provided by NVE Atlas web service (NVE, 2020).*

Some Prymnesiophyte species, have an unusually high demand for the thrace element selenium (Wehr et al., 1985; Wehr and Brown, 1985), others do not (Harrison et al., 1988). High selenite (Dahl et al., 1989), and/or cobalt (Granéli et al., 1993) concentrations in Baltic Current water, were one of the hypothesized causes of the *P. polylepis* HAB in the Kattegatt/Skagerakk-waters of 1988. Similarly, some haptophytes species increase toxicity

[7] As with temperature, the normal period for precipitation is based on the monthly average, measured from 1961 to 1991. The precipitation level is given as a relative percentage, with the average being 100% (Grinde and Mamen, 2019b)

towards grazers, as a result of nutrient depletion (Granéli and Johansson, 2003; Sopanen et al., 2006). Algae can also, in allelopathic interactions with other algae, produce toxins inhibiting the growth of their competitors (Wolfe and Rice, 1979; Dakshini et al., 1994).

Among other things, Rey et al. (1991) hypothesized, that the wintering of most of the Norwegian spring-spawning (NSS) herring stock in Ofot-/Tysfjorden - for several years, leading up to the HAB (Dommasnes et al., 1994) - could actively select for the blooming of *C. leadbeateri*. Compared with blooms of diatoms, which intensity is, to some degree, limited by the availability of nutrients (Brzezinski, 1985) and irradiance (Eilertsen and Frantzen, 2007). *C. leadbeateri* can ingest particles, and is believed to be mixotrophic (Edvardsen and Imai, 2006; Jones et al., 1994) - meaning it might utilize organic carbon for sustenance (Throndsen and Eikrem, 1991). It is also motile, giving it the ability to outcompete non- or less motile species in environments with vertically opposing resource gradients (Kamykowski and Zentara, 1977; Berdalet et al., 2014), and reducing its boundary layer limitation for nutrient uptake (Gavis et al., 1976; Berdalet et al., 2014).

1.6 million tonnes of wintering herring (Johannessen et al., 1991) - consuming oxygen and releasing waste products, combined with its natural mortality, decomposition and subsequent release of organic compounds in the fjords, leading to eutrophication and nutrient loading (Dommasnes et al., 1994) - could influence the ichthyotoxicity of algae (Shilo, 1967). A study by Johnsen et al. (1999), seemed to demonstrate that the addition of the polyamine putrescine - one of the by-products from bacterial decomposition of dead herring (Mackie et al., 1997) - enhanced *C. leadbeateri* haemolytic activity and cell biomass. Similarly, the feed and waste products from fish farms, might also have influenced its toxicity. It's important to note, that the toxicity experienced in the various HABs related to *C. leadbeateri*, have never been recreated in a laboratory setting.

The NSS herring stock would use the same wintering grounds until 2005 (Jourdain and Vongraven, 2017), when it shifted to an area north of Vesterålen (Huse et al., 2010). The stock of NSS kept moving further north, and during the 2019 HAB, the wintering grounds were outside the coast of Troms and Finnmark (Havforskningsinstituttet, 2019b).

3 Methodology

3.1 Sampling procedures and -locations

3.1.1 Microbial gDNA-extraction from fish gill samples

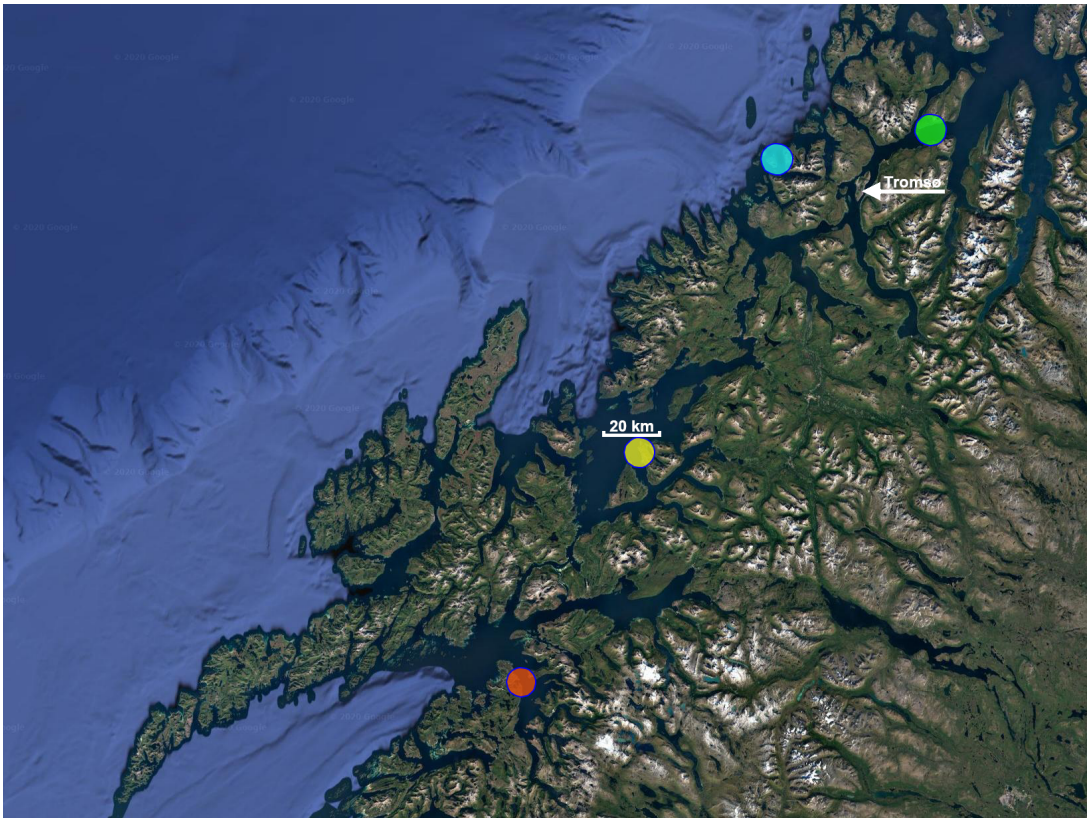

Figure 3.1: *Map showing locations from where we sourced HAB-afflicted fish gill-samples. Grøtsundet is marked in green, Kattfjorden in cyan, Astafjorden in yellow, and Tysfjorden in orange. Map template provided by SolarGIS web service (Šúri et al., 2011).*

The fish gills were sampled from the second branchial gill arch on the left side of the fish - in smaller fish, the adjacent gill arches would also be included - put in either a bag or a test tube. The samples were categorized as **dead**, **living** or **healthy** - depending on the state of the fish that was sampled - frozen using local amenities, before transport and final storage at -80 ^{o}C at UiT. If the fish was small enough for practical purposes ($<$500 g), we also received frozen, whole, dead fish. The samples were then further processed (section 3.4) and prepared for microbial gDNA-extraction (section 3.5.1).

3.1.1.1 Astafjorden (68^{o}54 N, 17^{o}06 E)

This locality is placed in the outer edge of Astafjorden, between Andørja and Ibestad. They experienced high HAB-related mortality on May 16-18th, killing a total of 157 655 salmon. The amount of fish killed, varied widely between the different pens, and they were also the locality farthest out in Astafjorden who experienced any HAB-related mortality. The fish sampled, weighed between 2-3 kg.

4 fish gill samples, from different pens, were collected on May 28th - during a routine veterinary inspection - with all the samples categorized as 'dead'. They were stored in a local freezer at -20 ^{o}C for 114 days, before being transported to Tromsø in a closed container with dry ice, then stored at -80 ^{o}C for 37 days before processing. These samples were not utilized in the first round of sequencing.

3.1.1.2 Tysfjorden (68^{o}12 N, 16^{o}08 E)

This locality is placed in the outer edge of Tysfjorden. They experienced high HAB-related mortality on May 18-20th, and May 30th-June 1st, as well as moderate mortality between May 21-27th, leading to the death of a total of 91 679 salmon. The fish sampled, weighed between 150-250g.

May 30th, 30 samples of whole, dead fish were collected by local workers. The day after, 20 fish gill samples were collected by a visiting fish health biologist. Both set of samples were stored at -20 ^{o}C for 14 days, before being transported to Tromsø - in a closed, isolated container with ice - where storage at -80 ^{o}C commenced.

The processing of 6 on-site-extracted gill samples classified as 'dead', and 6 samples classified as 'living', commenced after they spent respectively 138 and 141 days at -80 ^{o}C.

After 161 days, 18 samples from the batch of whole, frozen fish were thawed from -80 ^{o}C at 10 ^{o}C for 4 hours, the second and the adjacent branchial gill arches were immediately removed under sterile conditions, and put in 30 mL of sterile natural seawater, then refrozen at -80 ^{o}C. Until processing commenced, the samples were stored at -80 ^{o}C for respectively 2, 8 and 9 days, before being thawed at 4 ^{o}C for 14-16 hours. 6 out of 18 samples were chosen for further processing and sequencing, based on measurements of their 260:280 ratio and DNA-concentration (section 3.5.1).

3.1.1.3 Kattfjorden (69 ^{o}40, N 18^{o}11 E)

This locality is placed in Kattfjorden, outside Kvaløya. They experienced low HAB-related mortality on June 4-5th, killing 1 992 salmon. The fish sampled, weighed between 4-6 kg.

June 6th, we sampled 24 fish gill samples ourselves, immediately placing them in closed containers with dry ice and transporting them to Tromsø the same day - storing them at -80 ^{o}C. From salmon, we processed 14 samples: 6 were classified as 'healthy', 6 as 'dead', and 2 as 'living'. We also processed 4 gill samples from lumpsuckers (*Cyclopterus lumps*), for a total of 18 samples from this locality. The samples were processed in batches of 6 after spending 146, 155, and 156 days at -80 ^{o}C.

3.1.1.4 Grøtsundet (69^{o}50 N, 19^{o}31 E)

This locality is placed south of Reinøya, in Grøtsundet. They experienced no HAB-related mortality, though, interestingly, rather high cell counts of *C. leadbeateri* (Figure 4.2).

20 samples of whole fish, weighing between 150-250 g were put in a on-site freezer, between June 1 to 14th, by local workers, during routine dead fish hauling. These samples were transported to Tromsø June 14th, and stored at -80 ^{o}C. After 161 days, 6 samples were thawed at 10 ^{o}C for 4 hours, before removing the second and the adjacent branchial gill arches under sterile conditions. The gills were then transferred to tubes with 30 mL of sterile natural seawater at 4 ^{o}C, thawing for an additional 15 hours, before processing commenced.

3.1.2 *C. leadbeateri*-like Haptophyta from at-risk locations

During the 2019 HAB, we received unfixed water samples from at-risk locations in the Troms-region. These were gathered from both the surface, at 0.5-1 m, as well as further down, at 5-10 m. They were stored at 4 ^{o}C under low light conditions, for approximately 140 days, before we subjected them to a basic light-microscopy screen, to check for *C. leadbeateri*-like Haptophyta (Figure 4.9). Selected samples were then enriched (section 3.2.1), before we attempted to isolate individual *C. leadbeateri*-like haptophyta cells (section 3.3).

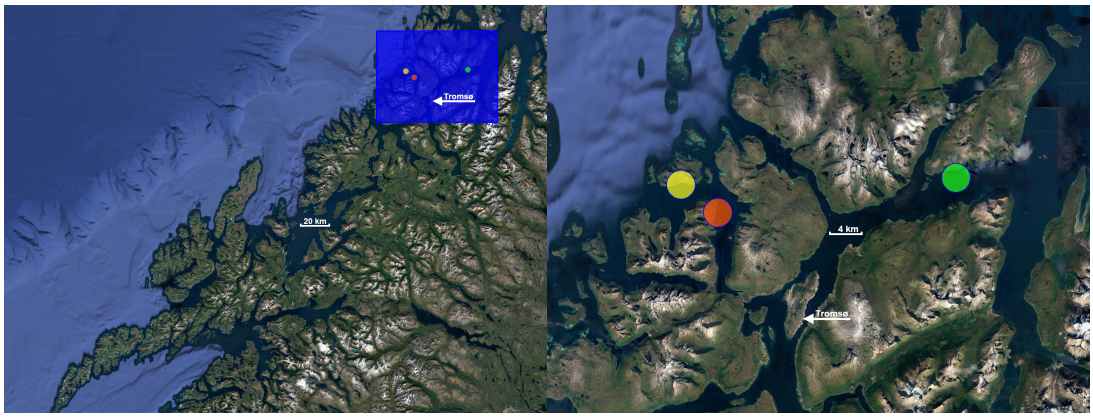

Figure 3.2: *Sampling locations for the isolation attempts of* C. leadbeateri*-like Haptophyta. The location in Grøtsundet is marked in green, Kattfjorden 1 in yellow, and Kattfjorden 2 in orange. Map template provided by SolarGIS web service (Šúri et al., 2011).*

3.1.2.1 Grøtsundet (69^{o}50 N, 19^{o}31 E)

This locality experienced no HAB-related mortality. The samples were collected at 1 and 10 m below the surface. Isolation attempts were performed on the samples collected at 10 m, cultivated on 'selenium-fortified F3'-medium (section 3.2.1). We also received gill samples from this locality (section 3.1.1.4).

3.1.2.2 Kattfjorden 1 (69^{o}49 N, 18^{o}31 E)

This locality experienced HAB-related mortality June 3rd and 4th. The samples were collected at 0.5 and 5m below the surface. Isolation attempts were performed on the samples collected at 0.5 m, cultivated on F4-medium.

3.1.2.3 Kattfjorden 2 (69^{o}47 N, 18^{o}39 E)

At the time of sampling, there was no fish at this locality. The samples from Kattfjorden 2 were collected at 0.5 and 5 m below the surface. Isolation attempts were performed on the samples collected at 0.5 m, cultivated on F4-medium.

3.1.3 Sampling from at-risk locations by Akvaplan-Niva

During the HAB, Akvaplan-Niva was commissioned by several salmon farmers in the Troms-region. They collected data between May 23rd - June 12th. In addition to water samples for enumeration of *C. leadbeateri* and nutrient analysis - for most localities - they also collected corresponding environmental- and CTD-data. The environmental data was

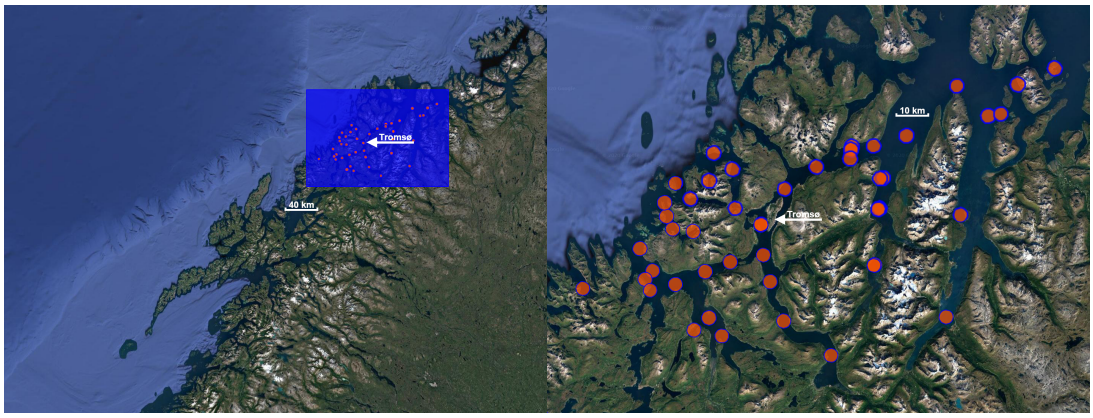

Figure 3.3: *Locations in Troms, marked with orange dots, where Akvaplan-Niva collected data between May 23rd and June 12th. The locations chosen, were based on risk assessments, made in concord with individual salmon farmers. None of these locations were continuously monitored. Map template provided by SolarGIS web service (Šúri et al., 2011).*

amassed through the use of tactile observation, thermometer, GPS, and a Secchi-disk. The CTD-instruments used, were all produced by SAIV AS[8].

Environmental data:

- Coordinates
- Wind Speed (m/s)
- Wave Height (m)
- Wind direction (N/E/S/W)
- Current direction (N/E/S/W)
- Cloud cover (None/Full - x/8)
- Air temperature (^{o}C)
- Transparency (m)
- Precipitation (None/Minute/Recurring/Constant)
- Colour of water (Blue/Green/Yellow/Brown/Red/Grey/Clear)

CTD-data:

- Salinity (ppt)
- Temperature (^{o}C)
- Fluorescence (μq/L)
- Turbidity (FTU)
- Oxygen saturation (%)
- Dissolved Oxygen (mg/L)
- Density (kg/m^3)
- Pressure (dbar)

For enumeration of phytoplankton, 25 mL of water was sampled, at depths ranging from 0-10 m, and conserved using 8 drops of Lugol. These were analyzed at NIVA Region West in Bergen. Between May 23 - 27th, the water samples were counted according to Norsk Standard (NS-EN 15204) - "*Water quality - Guidance standard on the enumeration of phytoplankton using inverted microscopy (Utermöhl technique)*". After May 28th, the protocol was simplified, only counting *C. leadbeateri*, and after June 2nd, supplemented with counts of *Phaeocystis* spp. in selected samples. Constrained by resources, they only prioritized the samples from the most at-risk locations for taxonomical enumeration.

[8]The CTD-instruments utilized, were likely the SD 204 (SAIV, Laksevåg, Norway), or an older model.

3.2 Cultivation

3.2.1 Enriching water samples from at-risk locations

The water samples with the highest observed abundance of *C. leadbeateri*-like Haptophyta, were first enriched in 3 replicate cultures. 100 mL from the samples were mixed 1:1 with F2-medium (Guillard and Ryther, 1962; Guillard, 1975) in 160 mL Nunc™ EasyYFlask™ cell culture flasks (Thermo Scientific, Waltham, MA, USA), turning it into F4-medium.

Since some *Chrysochromulina* species may require selenium, we split one replicate from each location. Thereafter, one of the split cultures was refilled 1:1 with TL-30 (Larsen et al., 1994) - a selenium-fortified medium. This made a total of 4 replicate cultures from each locality: 2 replicates of 200 mL F4; 1 replicate of 100 mL F4; and 1 replicate of 200 mL, F4 and TL-30 mixed 1:1 ('selenium-fortified F3-medium'). All the cultures were kept at 8-9^{o}C, illuminated at ∼60 µmol photons m^{-2} s^{-1}.

The viability of the cultivated samples were regularly checked under a microscope, by transferring ∼2 mL of sample with a 230 mm pasteur pipette onto a Nunc™ 4-well dish. After 55 days of cultivation, the samples with highest abundance of *C. leadbeateri*-like Haptophyta, were subjected to manual isolation through the use of a glass capillary pipette and inverted light microscopy (section 3.3).

3.2.2 Cultivation of *C. leadbeateri* (strain UIO-035)

UIO-035 is a strain of *C. leadbeateri*, isolated during the bloom of 1991. We obtained this strain from the Norwegian Culture Collection of Algae (NORCCA) September 12th, 2019. It was first cultivated in TL-30-medium (Larsen et al., 1994) at 8-9 ^{o}C in glass vials (Duran GL-18, Duran Group GmbH, Mainz, Germany), continuously illuminated at ∼60 µmol photons m^{-2} s^{-1}. For all further cultivation-efforts, the light and temperature conditions remained constant. After 48 days of preliminary cultivation, the strain was split into 6 new glass vials, with the purpose of keeping them as stock-cultures.

They remained as they were for 77 days, when 2 mL from each of the 6 stock-cultures were transfered into 40 mL flasks, together with 20 mL of L1-medium (Guillard and Hargraves, 1993) diluted 1:1 with 20 mL of sterile natural seawater.

After 4 days, 20 mL from each sample was mixed with 160 mL of F4-medium (Guillard and Ryther, 1962; Guillard, 1975), fortified with 20 nM of Selenium, as done by Johnsen et al. (1999). During each transfer, the flasks remained unstirred, and only the upper part of the cultures were relocated. As *C. leadbeateri* is highly motile, this was thought to reduce the amount of contaminants during each transfer.

After 10 days, one of the cultures was chosen to inoculate further cultivation - selected on the criteria of not being too dense, as the cultures grew faster than expected. 20 mL was transferred into larger, 400 mL Nunc™ flasks, together with 500 mL of F2-medium, fortified with 20 nM Selenium. They were then cultivated for 10 days and 20 hours (after we achieved 5 chlorophyll *a* measurements in the exponential growth phase), while continuously illuminated at ∼60 µmol photons m^{-2} s^{-1} at 8-9 ^{o}C.

The cultures of UIO-035 were harvested by pulling 125 mL from each culture onto 2.5 μm grade 5 qualitative filter paper (Whatman plc, Little Chalfont, United Kingdom), and subsequently filtering through an equal amount of sterile natural seawater, to 'wash out' smaller bacteria. Two controls were made, pulling 250 mL of sterile natural seawater onto the same filters. These were folded, wrapped in aluminium foil, and stored at -80 ^{o}C, until CTAB gDNA-extraction commenced 90 days later (section 3.5.2).

3.2.3 Measuring growth rate characteristics for UIO-035

Immediately after the cultivation of UIO-035 commenced, 15 mL, from each sample, was aseptically removed and preserved using two drops of Lugol's solution. This was repeated at the end of cultivation, though only 1 mL was removed, and the samples were diluted 1:14 with sterile natural seawater. Both the start- and end-point samples were counted manually under 200x magnification - following a protocol pioneered by Utermöhl (1931, 1958) - using a Axio Vert.A1 inverted microscope (Carl Zeizz AG, Oberkocken, Germamy), equipped with a LD A-Plan 20x objective lens and Ph1/0.4 condenser. 4-well dishes, with a diameter of 15.55 mm, a 'sedimentation area' of 190 mm^2, and volume of 2 mL, were used as counting chambers.

To reduce the effect of unequal settling in the counting chamber, each chamber was counted twice, in both vertical and horizontal transects. Each transect having a width of 0.5 mm, and length of 15.55 mm, crossing each other once, made the area of a single transect (a)

7.65 mm^2. Each start- and end-point sample was counted in 2 replicates, giving a total of 4 counted transects (N). Combining the two chambers, gave a total sedimentation area (A) of 380 mm^2, and a total volume (V) of 4 mL for the sedimented aliquot. The counts were performed after 24 hours of settling. The number of counting units per volume (L^{-1}) was then calculated by multiplying the number of units (n) counted in all the transects, with the coefficient C, which was obtained from Equation 3.1 (HELCOM, 2017).

$$C(L^{-1}) = \frac{A \cdot 1000}{N \cdot a \cdot V} \tag{3.1}$$

Treating the counts as a *Poisson* variable, an approximate 99% upper and lower confidence limit was found in accordance with Equation 3.2 (Ricker, 1937; Lund et al., 1958).

$$\begin{aligned} Upper\,limit &= n + 3.82 + 2.576 \cdot \sqrt{n + 2.2} \\ Lower\,limit &= n + 2.82 - 2.576 \cdot \sqrt{n + 1.2} \end{aligned} \tag{3.2}$$

3.2.3.1 Continuous monitoring

To measure chlorophyll a (Chl a), each day, ~15 mL of sample was withdrawn from each of the cultures. From this, an appropriate volume (V) - 0.5 - 5 mL - of sample, was filtered onto a GF/C-filter (Whatman plc, Little Chalfont, United Kingdom), in replicates of 3 for each culture. We used 5 mL of 96% ethanol as an extraction agent - following a modified version of Holm-Hansen and Riemann (1978). The samples were then kept at 4 ^{o}C under dark conditions, for 14-16 hours. Afterwards, they were carefully homogenized, before decanting the supernatant into quartz cuvettes. Concentration values were measured using a TD-700 fluorometer (Turner Designs, Sunnyvale, CA, USA). Controls were performed before each set of measurements, by subjecting 5 mL 96% ethanol to the same protocol. These were used as blanks for each set, and subtracted from all the ensuing measurements. After the initial measurement (R_a), each sample was subjected to 2 drops of 10% HCl, to acidify the sample, carefully homogenized, and remeasured (R_b). The calibration constant (K) was set to 0.003439, and Chl a was calculated in accordance with Equation 3.3.

$$Chl\,a\,(\mu g \cdot L^{-1}) = \frac{k(R_a - R_b)}{V} \tag{3.3}$$

An exponentially growing culture can be mathematically modelled with a 1st order rate equation: $dN/dt = \mu \cdot N$, where (μ) is the growth constant/specific growth rate, t is the time, and N is the number of cells, or a quantity proportional to this (Hoogenhout and Amesz, 1965). This is only part of the standard, basic form of the logistic equation, used to describe population dynamics in ecology (Rockwood, 2015), which also includes the parameters initial population size (N_0) and carrying capacity (K). Growth characteristics for all cultures, was obtained using the 'Growthcurver' package in R (Sprouffske and Wagner, 2016), which fitted the Chl *a*-measurements onto Equation 3.4.

$$N_t = \frac{K}{1 + (\frac{K - N_0}{N_0}) \cdot e^{-\mu t}} \tag{3.4}$$

3.3 Isolation of *C. leadbeateri*-like Haptophyta from at-risk locations

After 55 days of cultivation, the enriched samples - from at-risk locations - with the highest relative abundance of *C. leadbeateri*-like Haptophyta, were subjected to manual isolation, through the use of a glass capillary pipette and inverted light microscopy (Andersen and Kawachi, 2005). ~50 μL of culture were transferred and diluted into 20 mL of sterile natural seawater in 40 mL Nunc™ flasks. From this dilution, we transferred enough sample to barely cover the bottom in one of the chambers in a 4-well dish. The three remaining chambers were similarly filled with minute amounts of sterile natural seawater.

Individual cells were identified at 400x magnification, using a Primo Vert™ inverted microscope (Carl Zeizz AG, Oberkocken, Germamy), equipped with a Zeizz LD Plan-Achromat 40x objective lens and a Ph2/0.4 condenser. Once identified, and before performing the isolation at 40x magnification, the objective lens was changed to Zeizz Plan-Achromat 4x, and the condenser to Ph1/0.2.

The process proceeded by dipping the pipette into one of the chambers containing sterile natural seawater, before guiding it onto the chamber containing sample, sucking up

individual cells, through capillary action. The microscope was reoriented to the chamber which sourced the sterile natural seawater, focusing on the pipette tip, before gently adding pressure until the transfer of a singular cell was observed. After completing transfers to all three chambers, they were filled up with F5-medium (∼2 mL).

The chambers containing the (presumed) isolated algae were incubated in the dark at 8-9 ^{o}C for 18 days, before being relocated and illuminated at ∼60 µmol photons m^{-2} s^{-1} for 32 days. As the chambers containing the samples were not sealed, a significant volume of media had evaporated. To ease microscopy when assessing the success of the isolation attempts, the chambers were refilled with sterile natural seawater.

After spending a *further* 143 days under dark conditions at 8-9 ^{o}C, the viability of the originally enriched samples from at-risk locations were rechecked - reassessing the abundance of *C. leadbeateri*-like Haptophyta.

3.4 Preparation of fish gill samples for microbial gDNA-extraction

The fish gill samples were prepared for processing by placing them in individual 50 mL polypropylene centrifuge tubes (Thermo Fisher Scientific, Waltham, MA, USA), together with 30 mL of sterile natural seawater - thawing at 4 ^{o}C over night.

After thawing for 14-16 hours, the fish gills were vigorously vortexed for 3 minutes each. Thereafter, they were filtered through a plankton net (mesh size 200 μm), on top of a new 50 mL tube, taking care to keep the fish gill solids remaining in the original tube. This was repeated, with the addition of funnels and by using a smaller plankton net (mesh size 20 μm). We then gently shook the samples, until we had filtered >25 mL of liquid.

47 mm magnetic filter funnels (Pall Corporation, Port Washington, NY, USA) were placed on top of a 6-channel filtration unit (Millipore, Burlington, MA, USA), utilizing 0.2 μm polycarbonate filters (Whatman plc, Little Chalfont, United Kingdom). Before pouring in the sample, we sealed off the funnels with parafilm. The filtration unit was supplied with -60-70 kPA vacuum. The filtration, in some cases, took upwards of 10 hours to complete (Figure 4.15). When finished, the 0.2 μm polycarbonate filters were carefully folded - twice over, diagonally - wrapped in aluminium foil, and stored at -80 ^{o}C.

For negative controls, 6 replicates were made by repeating the procedure with sterile natural seawater. The natural seawater was sterilized sequentially through a UV-filter, pasteurized, before being pulled through a 0.2 μm polycarbonate filter - a treatment performed on all the sterile natural seawater we used. For positive controls, we split a *C. leadbeateri* monoculture into 6 replicates of 10 mL, filtering them onto 0.2 μm polycarbonate filters, folded and wrapped in aluminium foil, then stored at -80 ^{o}C.

3.5 Microbial gDNA-extraction

3.5.1 Fish gill DNA-isolation, amplification, and sequencing

To prepare the fish gill samples for Illumina MiSeq sequencing, gDNA was first isolated, using the DNeasy PowerWater Kit (Qiagen, Hilden, Germany). The DNA concentration and -purity was then assessed using a NanoDrop1000 Spectrophotometer (Thermo Scientific, Waltham, MA, USA). Purity was assessed through the 260/280 and 260/230 ratio. Pure DNA typically yield a 260/280 ratio in the range of 1.7 - 2.0 (Burtis and Bruns, 2014), and a 260/230 ratio of 1.8-2.2 (Desjardins and Conklin, 2010).

Subsequently, the gDNA was amplified through a polymerase chain reaction (PCR), accompanied by the primers 515F-806R and 1391F-EukBR, for prokaryotes and microeukaryotes respectively, adhering to the protocol of the Earth Microbiome Project (Thompson et al., 2017).

515F (5'-GTGYCAGCMGCCGCGGTAA-3' Parada et al. (2016)), and 806R (5'-GGACTACNVGGGTWTCTAAT-3' Apprill et al. (2015)) targets the V4 regions of the 16S SSU rRNA in prokaryotes (Caporaso et al., 2011).

1391F (5'-GTACACACCGCCCGTC-3' Lane (1991)), and EukBR (5'-TGATCCTTCTGCAGGT-TCACCTAC-3' Medlin et al. (1988)) targets the V9 region of the 18S SSU rRNA in eukaryotes (Stoeck et al., 2010).

A PCR test run and assessment through agarose gel electrophoresis, implied the potential presence of PCR-inhibitors (Figure 4.13). Hence the isolated DNA was subjected to the OneStep™ PCR Inhibitor Removal Kit (Zymo Research, Irvine, CA, USA) before any further amplification.

The amplified DNA was shipped to the Environmental Sample Preparation and Sequencing Facility (ESPSF) at the Argonne National Laboratory (Lemont, IL, USA), to standardize

our prepared libraries and undergo Illumina MiSeq sequencing, in accordance with the Earth Microbiome Project protocol (Thompson et al., 2017).

3.5.2 UIO-035 HMW CTAB gDNA extraction

High molecular weight (HMW) DNA was extracted through a modified hexadecyltrimethylammonium bromide (CTAB)-based protocol, utilized by Puppo et al. (2017) and Villain et al. (2017). Instead of obtaining biomass through careful centrifugation, we obtained ours from the 2.5 μm grade 5 qualitative filter paper (Whatman plc, Little Chalfont, United Kingdom). We also utilized wide-mouth pipettes when manipulating the aqueous phase. QC was performed by subjecting the samples to agarose gel electrophoresis with a BenchTop 1kb Plus DNA ladder, and the NanoDrop® 1000 Spectrophotometer.

3.5.2.1 Estimating bacterial contamination

A rough estimate of bacterial contamination in the cultures, were calculated by assessing them under epifluorescence microscopy, using a 4',6'-diamidino-2-phenylindolestain (DAPI)-stain (Porter and Feig, 1980). From each of the 4 cultures, 5 mL (V) of sample was filtered onto 0.2 μm polycarbonate filters (Whatman plc, Little Chalfont, United Kingdom), using 5 mL of sterile natural seawater as control. The filters were cut into ~4x10 mm rectangles, stained with DAPI-solution (1 mg/mL), incubated in the dark for 5 minutes, before being rinsed in sterile natural seawater, and placed onto a microscopy slide for immediate examination under a DM LB2 epifluorescence microscope (Leica Microsystems, Wetzlar, Germany) using a Leica 40x N Plan objective lens. Controls were made by repeating the process with two samples of sterile natural seawater. The controls were used as blanks, to assess background contamination on the filters, and subtracted from each of the counts.

At 400x magnification, all (n) colony forming units (CFU) in 10 fields of vision (N) of 0.25 mm^2 (a) were counted, out of a total sedimentation area of 12 566 mm^2 (A). Bacterial contamination was calculated by multiplying the number of CFU counted with the coefficient C, obtained in Equation 3.1, and approximate 99% confidence limits were established in accordance with Equation 3.2.

3.6 Data processing and analysis

3.6.1 Processing data collected by Akvaplan-Niva

When procuring samples and measurements, workers would document this in a series of cross-referencing forms, often filled out by hand and scanned into a PDF. In the environmental data, there would be reference to at what time and which of the CTD-instrument were utilized. Concurrent to this, most of the uploaded CTD-measurements were accompanied by a form, identifying which measurements corresponded to which locality. Until now, there had been no centralized effort to combine this information.

A total of 5 different CTD-instruments were utilized, two of which only measured fluorescence, and two only measuring turbidity. For two of the instruments, the internal clock was off by 3 hours, the other three being off by 2 hours. This was corrected in the final data set. In the cases were air temperature was not recorded in the environmental data, these were transcribed from the CTD measurements.

In the final data set, each record - separated by date and location - contained, if possible, the combined information from the environmental, taxonomical, and CTD-data. Each record also contained a citation to the file from which each variable was sourced. Included in the final data set, were CTD-measurements from 3 and 10 m below the surface, except for some of the measurements taken before May 28th, where the CTD-data further included, corresponded to the depth from which the taxonomical enumeration had been performed. The CTD-measurements at a select depth, taken on the way down and up, were equally weighted. To make the CTD-measurements correspond to a given depth, the weighted arithmetic mean of two measurements - taken right above ($m1$), or below ($m2$), the given depth (y) - were calculated in accordance with Equation 3.5.

$$x \cdot m1 + (x - 1) \cdot m2 = y \tag{3.5}$$

3.6.2 Data manipulation and reproducibility

All analysis were carried out using R version 3.6.3. Datasets were manipulated using the packages 'tidyr' (Wickham and Henry, 2020), 'dplyr' (Wickham et al., 2020), 'reshape2' (Wickham), 'purrr' (Henry and Wickham, 2020), and 'stringr' (Wickham, 2019). The statistical analysis was further enhanced by the 'PupillometryR'- (Forbes, 2020), 'Rmisc'- (Hope, 2013), 'statmod'- (Giner and Smyth), 'car'- (Fox et al., 2020), and 'growthcurver' (Sprouffske and Wagner, 2016) -packages. Plots were made using 'ggplot2' (Wickham, 2016), 'ggforce' (Pedersen, 2019), 'ggpubr' (Kassambra, 2020), 'gghalves' (Tiedemann, 2020), 'ggmap' (Kahle and Wickham, 2013), and 'scales' (Wickham and Seidel, 2020) - with the addition of 'extrafont' (Chang, 2014) and 'RColorBrewer' (Neuwirth, 2014) to provide a uniform aesthetic.

All data and analysis presented throughout this thesis, is publicly available through the Open Science Framework (OSF)[9].

[9] https://osf.io/42ebt/

4 Results

4.1 Enumeration of *C. leadbeateri* in Troms

During the 2019 HAB, Akvaplan was commissioned by several individual salmon farmers in the Troms-region. To our knowledge, nobody has yet commissioned them to perform a meta analysis of this data. As such, we were granted full access to all the data they collected, pertaining to the 2019 HAB.

Shown in Figure 4.1, are the daily *C. leadbeateri* cell counts and fish mortality at a location in Kattfjorden. It shows a marked increase and subsequent decline in cell counts, with coetaneous fish mortality. Figure 4.2 shows the daily cell counts at a unaffected locality in Grøtsundet - from which we also collected gill samples (section 3.1.1.4).

Figure 4.3 shows the max density of *C. leadbeateri* at each locality in the Troms-region - at different depths - in the period May 28th-June 12th, 2019. The highest cell counts were observed in the inner part of Balsfjorden - May 28th - where it's estimated that there were **48 607 600** cells/L, 3 m below the surface. Concurrently - at the same time and location - at 10 m below the surface, there was 'only' an estimated **5 641 650** cells/L. Further, in Figure 4.4 a and b, we've illustrated all the cell counts at 3 and 10 m, sampled in the period May 28th-June 12th, 2019. Here, only samples which were counted at both 3 and 10 m are included. The figures suggest, that during the 2019 HAB, there was a higher density of *C. leadbeateri* at 3 m below the surface, compared with 10 m,

Figure 4.5 is a heatmap that showcases the difference between *C. leadbeateri* counts at 3 and 10 m below the surface, for each sampling, at each location, in the period May 28th-June 12th, 2019. In 97 out of 109 observations, there was a higher density of *C. leadbeateri* at 3, compared with 10 m. In Figure 4.6, the difference in cell counts at 3 and 10 m, at different dates, is plotted against the concurrent water density difference - which we deemed indicative of the pycnocline strength and -existence between the two sampling depths. On top of this, we've showcased a series of linear regression models - correlating 'pycnocline strength' with the observed differences in cell density at 3 and 10 m for a set of timeseries. As seen in Table 4.1, the correlation between pycnocline strength and differing cell counts, were strongest in the period May 28th-June 5th.

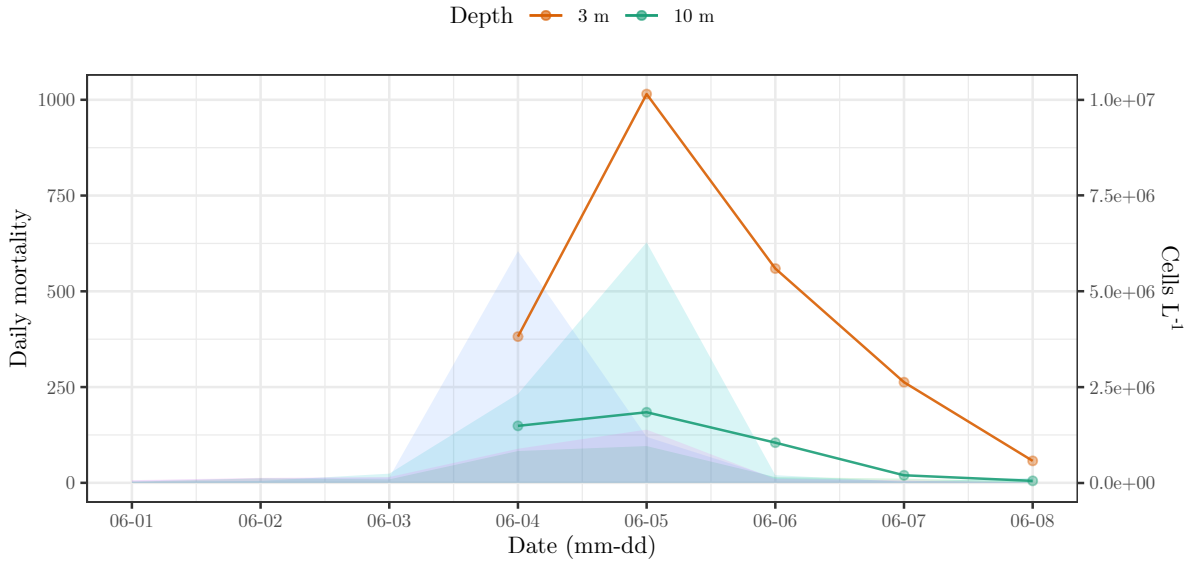

Figure 4.1: Daily fish mortality and concurrent* C. leadbeateri *cell counts in Kattfjorden. *Showcasing daily mortality - in different fish pens - from June 1st-8th, 2019. Ticks on the left Y-axis denote the daily mortality, while ticks on the right is concurrent* C. leadbeateri *cell counts. Note that there were no enumeration of* C. leadbeateri *on this locality until June 4th. Made using the 'ggplot2' and 'RColorBrewer' package (Wickham, 2016; Neuwirth, 2014) in R.*

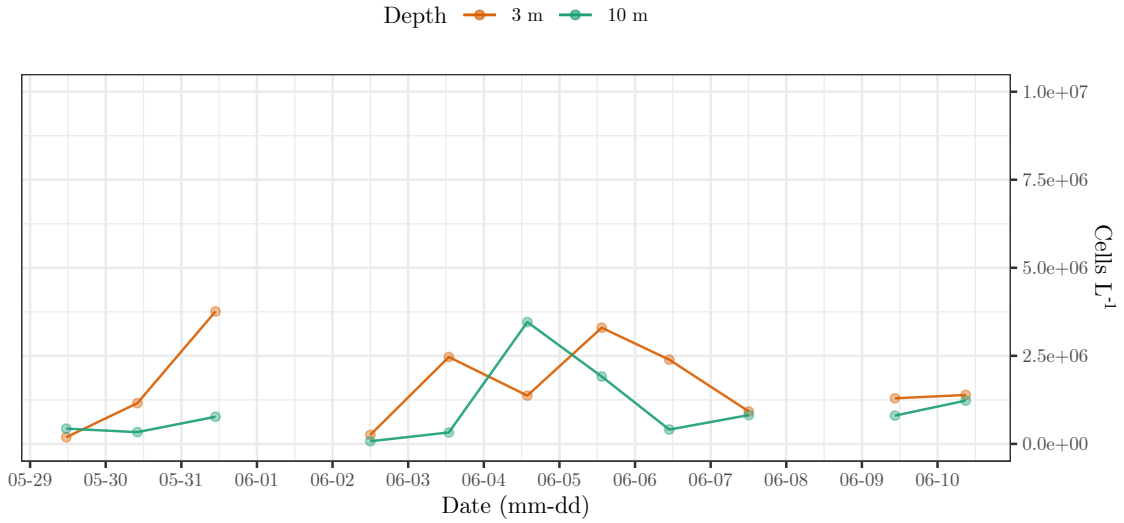

Figure 4.2: Daily* C. leadbeateri *cell counts at a locality in Grøtsundet. *Includes the samples enumerated from May 29th-June 10th, 2019. In contrast with the figure above, the temporal sample resolution is by hour, not by date. Made using the 'ggplot2' and 'RColorBrewer' package (Wickham, 2016; Neuwirth, 2014) in R.*

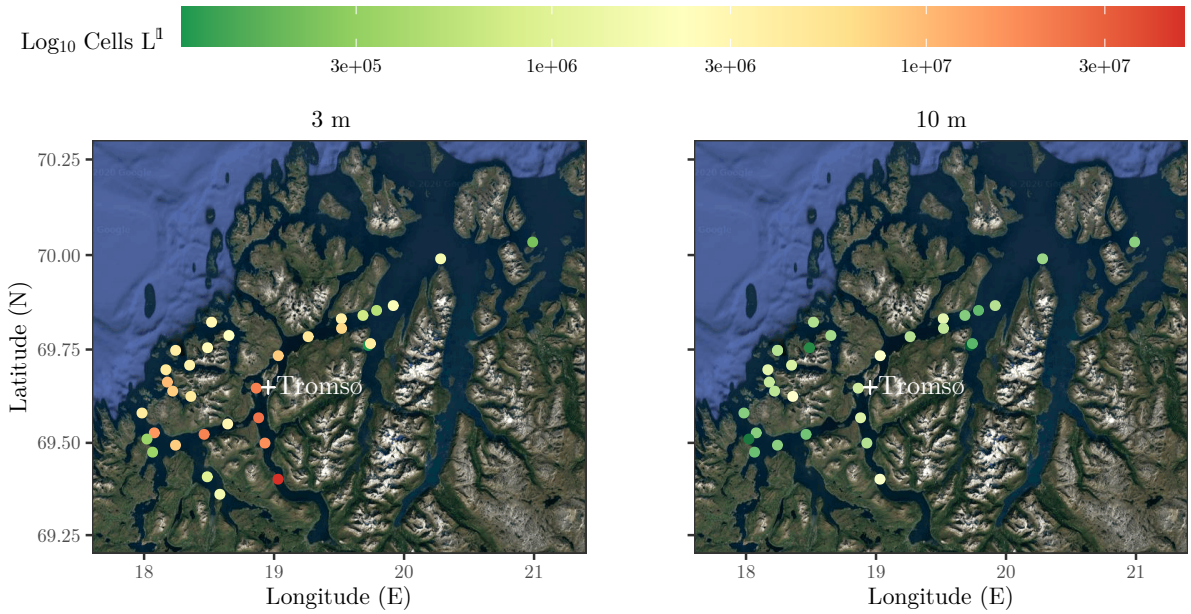

Figure 4.3: The densest cell counts of* C. leadbeateri *for each location in the Troms-region. *Only the max count for each location sampled between May 28th-June 12th 2019 is included. The colour scheme is on log_{10}-scale, with red representing high and green low cell counts. Made using the 'ggplot2', 'ggmap', 'ggpubr' and 'RColorBrewer' package (Wickham, 2016; Kahle and Wickham, 2013; Kassambra, 2020; Neuwirth, 2014) in R.*

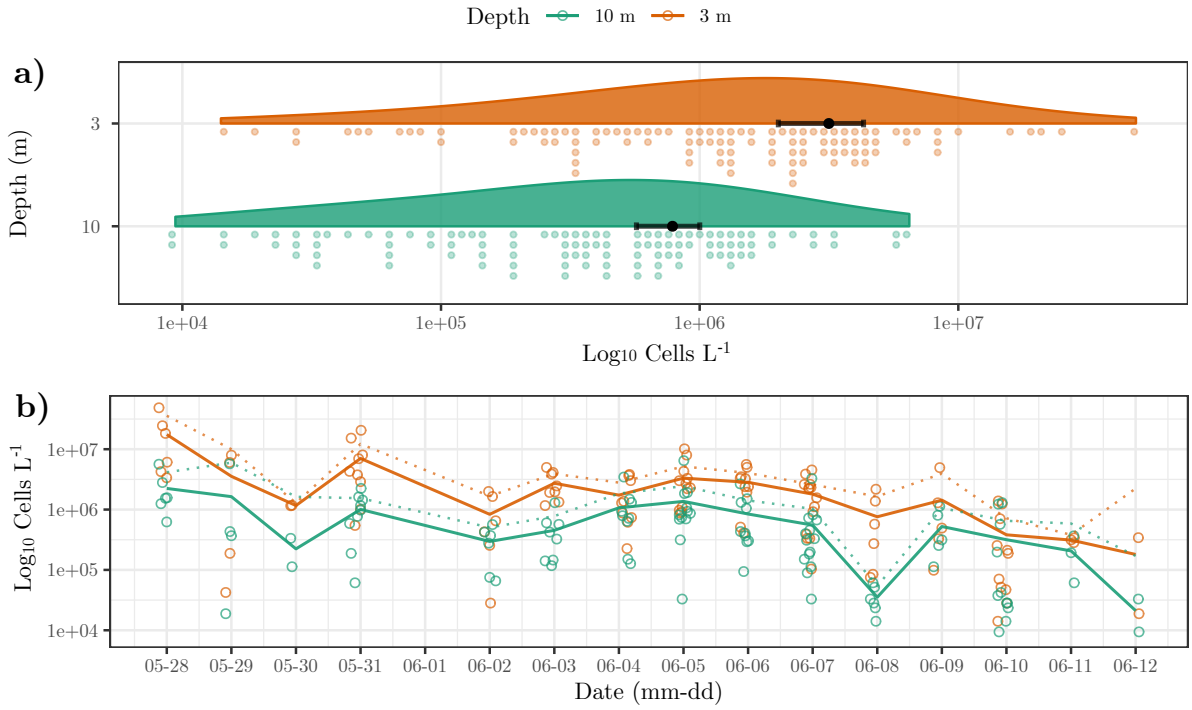

Figure 4.4: Cell counts of* C. leadbeateri *at 3 and 10 m. *Only includes cell counts with concurrent measurements at both depths, sampled between May 28th-June 12th 2019. Note that cell density is shown on a log_{10}-scale.* ***a****) raincloud plot (Allen et al., 2019) showcasing all cell counts at both depths. Each dot represent a single enumeration. Black error bar denotes the arithmetic mean and 95% confidence interval.* ***b****) is a time-series, where solid lines denotes the mean of all enumerations at a certain depth, while dotted lines is the upper 95% confidence interval. Made using the 'ggplot2', 'PupillometryR', 'ggpubr', and 'Rmisc' package (Wickham, 2016; Forbes, 2020; Kassambra, 2020; Hope, 2013) in R.*

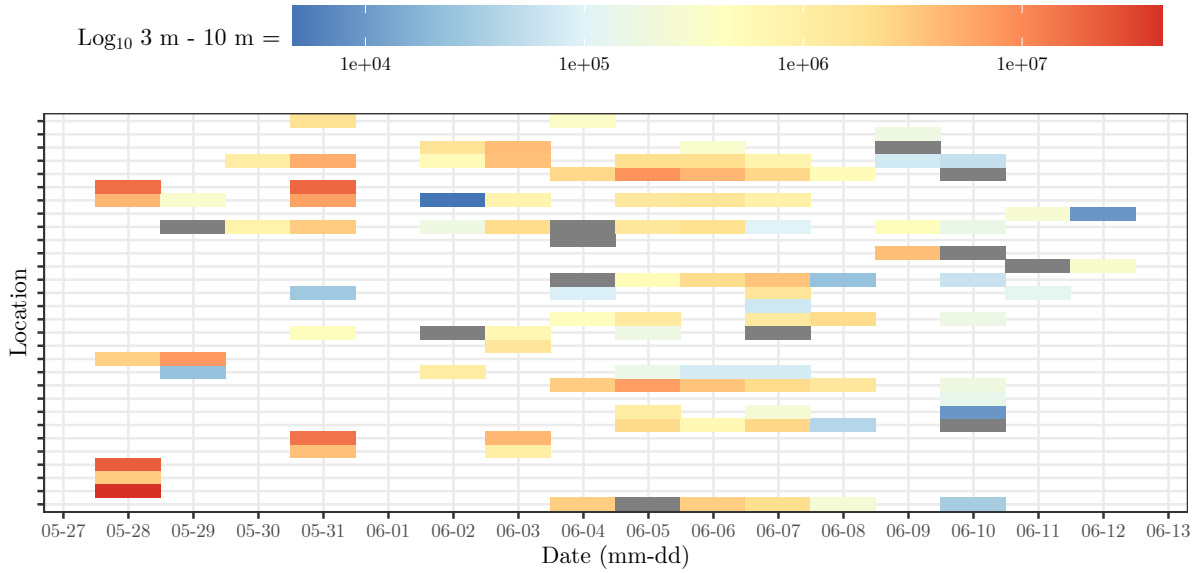

Figure 4.5: The difference between* C. leadbeateri *cell counts at 3 and 10 m. *The colour scheme is on a log_{10}-scale, with red representing high and blue a low difference in cell counts. Gray denotes there being a higher density at 10 m, compared with 3 m. Made using the 'ggplot2' and 'RColorBrewer' package (Wickham, 2016; Neuwirth, 2014) in R.*

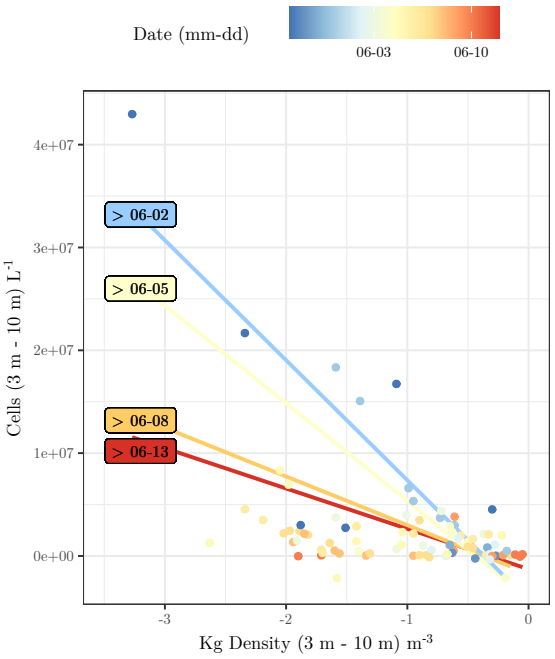

Figure 4.6: Correlation between pycnocline strength and difference in* C. leadbeateri *cell counts at 3 and 10 m. *Color scheme is based on sampling date. Pycnocline strength is calculated as the density difference at 3 and 10 m. Linear correlation is calculated for the timeseries: May 28th-June 2nd, -5th, -8th, and 13th. Made using the 'ggplot2' and 'RColorBrewer' package (Wickham, 2016; Neuwirth, 2014) in R.*

Table 4.1: Linear regression models for the different CTD-parameters. *β denotes the slope of the linear model, SE the standard error, t the t-statistic, and P the p-value. The rows compiled together between the line breaks represent the parameters from multiple regression models - besides the last rows, which showcases singular linear regression models for the timeseries shown on the left figure.*

Variable	β	***SE***	***t***	***P***
Salinity	-2.36E+08	5.86E+07	-4.021	1.27E-04 ***
Temp.	4.17E+07	1.04E+07	4.027	1.24E-04 ***
Opmg	-1.53E+05	1.09E+06	-0.140	8.89E-01
Density	2.97E+08	7.46E+07	3.975	1.50E-04 ***
Salinity	-2.78E+06	1.29E+06	-2.164	3.33E-02 *
Temp.	1.03E+06	1.73E+06	0.596	5.53E-01
Salinity	-3.43E+06	6.91E+05	-4.965	3.44e-06 ***
Temp.	4.20E+06	9.55E+05	4.395	3.15e-05 ***
Density by date:				
> 06-13	-3.92E+06	7.92E+05	-4.954	3.60e-06 ***
> 06-08	-4.73E+06	9.36E+05	-5.054	3.32e-06 ***
> 06-05	-9.51E+06	1.39E+06	-6.828	6.38e-08 ****
> 06-02	-1.17E+07	1.76E+06	-6.637	5.71e-06 ***

4.2 Growth characteristics

In addition to establishing cell counts for the cultures harvested for CTAB-extraction (section 4.4.1), we also sought to verify that the cultures were harvested in the exponential growth phase. Originally, the main goal was to establish baseline growth phenotype characteristics for the strain UIO-035, to compare with the strains isolated from our enriched water samples (section 4.3). This, unfortunately, was beyond the scope of this thesis - as none of the isolation attempts proved successful.

Individual Chl *a*-measurements in the exponential growth phase and extrapolated growth curves are illustrated in Figure 4.7. As shown in Table 4.2, there were no statistical significant differences in the calculated growth curves. In addition, the combined specific growth rate for all the samples, had a lower standard error ($\mu\, SE$) than the individual, calculated specific growth rates. In Table 4.3 are the growth phenotype characteristics of the calculated growth curves (Equation 3.4), in addition to the cell counts for all cultures. In Figure 4.8, are the combined growth curve for all the samples. All cell counts were also combined in this figure, despite some being classified as significantly different (Table 4.3).

Table 4.2: Pairwise comparison between UIO-035 growth curves *by the permutation test compareGrowthCurves function from the'statmod' package (Giner and Smyth) in R. The estimated P-values were the result of* 10 000 *permutations for each group, using the mean t-statistic of the growth curve for each sample.*

Groups		P	
		Estimated	*Adjusted*
S1	S2	0.40	0.60
	S3	0.20	0.60
	S4	0.10	0.60
S2	S3	0.20	0.60
	S4	0.10	0.60
S3	S4	0.10	0.60

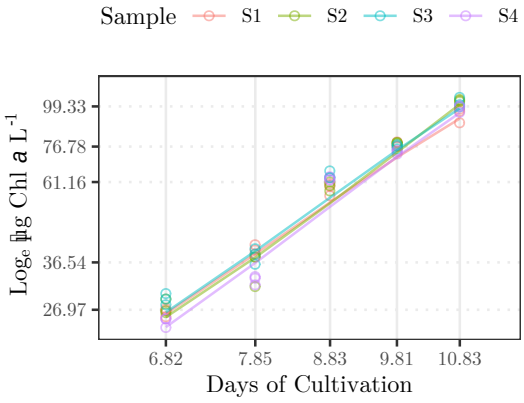

Figure 4.7: log$_e$-scale plot for the estimated growth curves *and the last 5 Chl* a*-measurements in the exponential growth phase. Ticks on the Y-axis showcase the mean of the combined samples. Made using the 'ggplot2' package (Wickham, 2016) in R.*

Table 4.3: Growth characteristics for cultures of UIO-035. *μ is specific growth rate, and μSE is its standard error - both values obtained through the SummarizeGrowthByPlate function from the 'growthcurver' package (Sprouffske and Wagner, 2016) in R. Upper and lower 99% confidence interval is extrapolated from Equation 3.2. Groups of start- and end counts which significantly differ ($p < 0.01$), are marked in either* regular, ***bold***, *or italic font. To adjust for dilution, the end-counts ($t = 10.826$) are multiplied with 15. The combined growth curve values and counts are shown in blue.*

Sample	μ	N_0	K	$SE\mu$	Start 99% CI		End 99% CI	
					Upper	*Lower*	*Upper*	*Lower*
S1	0.46	1.36	175.53	0.0260	**3 470**	**3 167**	46 238	41 947
S2	0.41	1.69	331.15	0.0256	**3 255**	**2 962**	45 562	41 303
S3	0.45	1.38	206.39	0.0265	2 861	2 586	46 207	41 918
S4	0.47	1.12	204.05	0.0381	*2 531*	*2 272*	**52 299**	**49 431**
Combined	0.44	1.45	223.26	0.0153	11 831	11 270	185 884	177 281
			Cells L^{-1} ($C = 716$)		9.18E+06	8.75E+06	1.44E+08	1.38E+08

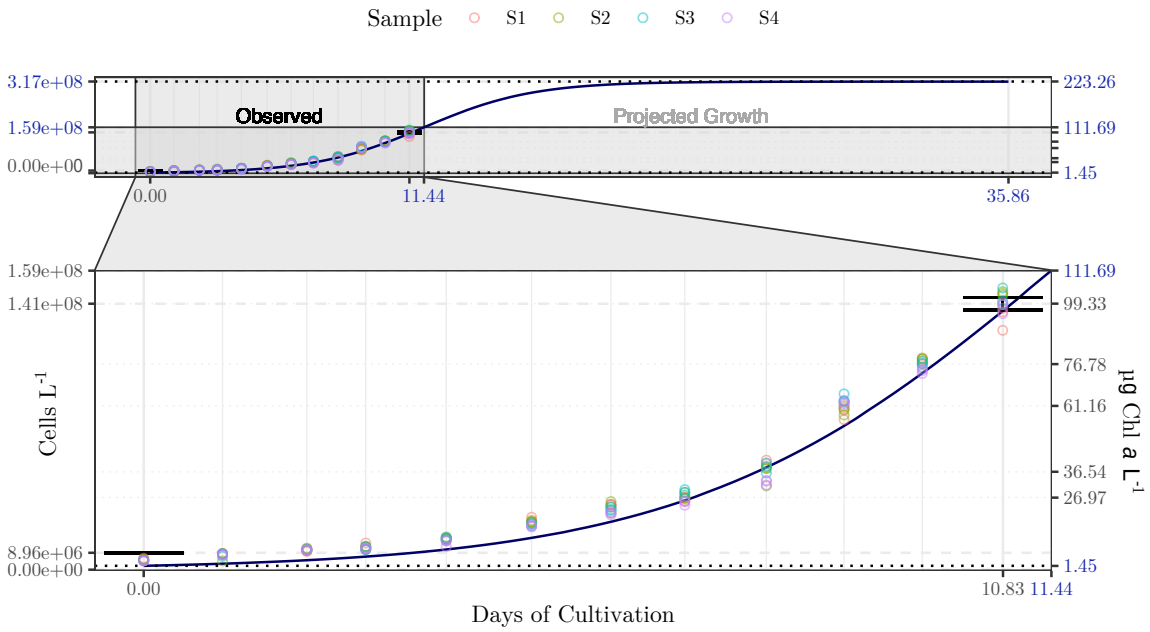

Figure 4.8: Projected growth curve for the combined samples. *The second, right Y-axis (μg Chl a L^{-1}) is fitted onto the plot by a factor of* 1 419 276.23*, matching the mean of all Chl* a*-measurements with the calculated cell density of the combined samples at $t = 10.83$. Note that zero on both axis harmonize. Blue ticks on the y- and x-axis relate to the values N_0, K, inflection point (t_{mid}) and $t_{\sim K.00}$ from the calculated growth curve. t_{mid} is used as the limits for the enhanced portion of the plot. Black ticks on the right Y-axis showcase the mean of the last 5 Chl* a*-measurements of the combined samples. Confidence interval of both start- and end count is shown as horizontal black lines at $t = 0$ and* 10.83*. Made using the 'ggplot2' and 'ggforce' package (Wickham, 2016; Pedersen, 2019) in R.*

4.3 Isolation of *C. leadbeateri*-like Haptophyta

By isolating *C. leadbeateri*-like haptophyta from at-risk locations, we sought to compare the isolates, initially to verify that they were the same species. Successful isolation and initial comparison through growth rate characteristics, unfortunately, proved beyond the scope of this thesis.

When identifying *C. leadbeateri*-like Haptophyta cells for isolation, we looked for circular, ∼Ø3-8 μm, motile cells, with 2 or 3 discernible flagella/haptonema (Figure 4.9). In total, 81 isolation attempts - 27 from each location - were performed. When screening these for live cells 32 days later, we found none. When surveying the enriched cultures, 198 days after their initial enrichment, they all still contained *C. leadbeateri*-like Haptophyta (Figure 4.10), in addition to other algae.

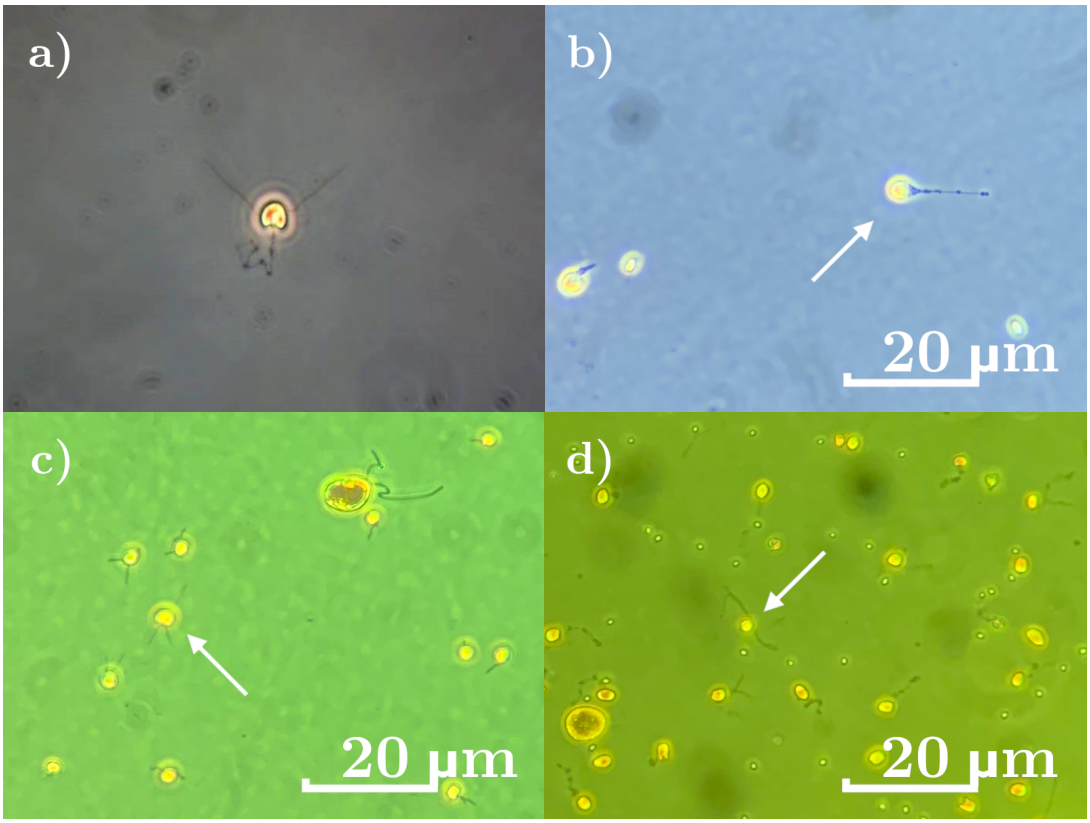

Figure 4.9: Light microscopy pictures of* C. leadbeateri*-like Haptophyta in the enriched cultures *- before initial isolation attempts:* ***a)*** C. leadbeateri *in water samples collected outside Rinøyvåg during the 2019 HAB (Havforskningsinstituttet, 2019a) - reprinted with permission from HI;* ***b)*** *Cell of similar size to* C. leadbeateri*, found in abundance in water samples collected in Grøtsundet;* ***c)*** *Cell of similar size, and, in all likelihood, having two flagella and one haptonema, collected in Kattfjorden (1);* ***d)*** *Cell of similar size, with 2-3 flagella/haptonema, collected in Kattfjorden (2).*

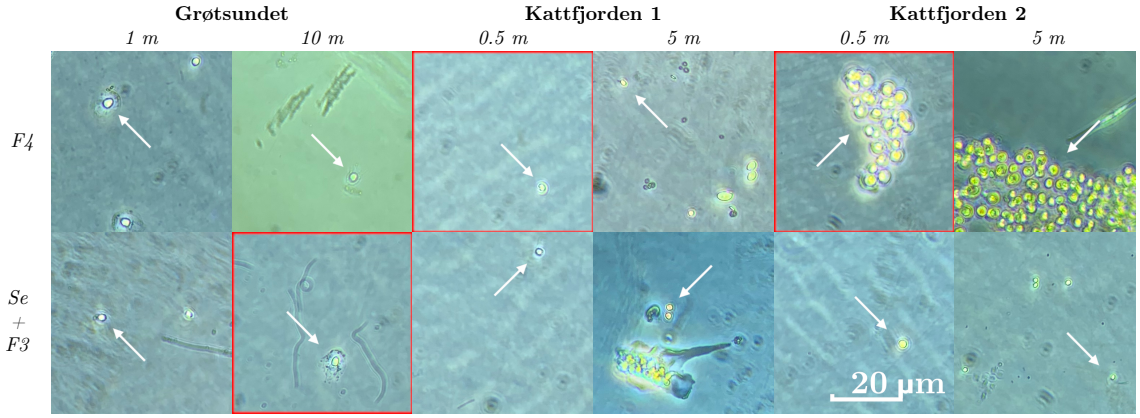

Figure 4.10: A survey of the enriched water samples *(400x magnification) - re-checked 198 days after their initial enrichment. Red frames denote the cultures from which the initial isolation attempts were made. Note, that the cells pictured above, were not subjected to isolation, but rather the 'most'* C. leadbeateri*-like cells found remaining in the unstirred cultures.*

4.4 Microbial gDNA-extraction

4.4.1 HMW CTAB gDNA extraction from UIO-035

Gaining a genome informed understanding of *C. leadbeateri*'s potential toxin production, is a long term and grand goal for researchers, following up on the 2019 HAB. Hence, a protocol for isolation of high molecular weight (HMW) gDNA is necessary. Full genome sequencing, assembly and annotation, were beyond the intermediate scope of this thesis. Nevertheless, the quality control procedures we performed, could help guide future work.

After the first round of extractions, it became apparent that the DNA-yield was much lower than expected. Further extractions were deemed futile, so the procedure was only performed on two of our samples (S1 and -2). Included as positive controls, and partaking in the same round of extraction, are two samples from the diatom *Porosira glacialis* (**P**3 and -4) strain CCAP 1060/9 (CCAP, 2009). **P**3 underwent the same harvesting protocol as described in section 3.5.2, utilizing a 5 μm polycarbonate filter; while **P**4 was harvested through centrifugation, then immediately flash frozen with liquid nitrogen.

Quality control measurements are shown in Table 4.4, and the agarose gel in Figure 4.11. The gel seemed to indicate that the DNA-fragments were larger than 20 000 bp. Epifluorescence microscopy images of the DAPI-stained cultures is illustrated in Figure 4.12. The resulting estimate of Cells L^{-1} and relative bacterial contamination (%) in the combined cultures, are illustrated in Table 4.5.

***Table 4.4: Quality control of the CTAB-extracts**, showcasing DNA-concentration, and the 260/280 and 260/230 ratio. Samples S1-2 are.* C. leadbeateri, *while **P**3-4 are* P. glacialis.

Sample	[DNA]	260	
	$ng \cdot \mu L^{-1}$	*280*	*230*
S1.1	27.1	1.65	2.06
S1.2	9.4	1.85	1.38
S2.1	8.9	2.05	1.59
S2.2	13.1	1.65	1.53
P3.1	408.0	1.89	2.34
P3.2	293.2	1.91	2.23
P4.1	36.0	2.04	1.91
P4.2	28.7	1.86	1.76

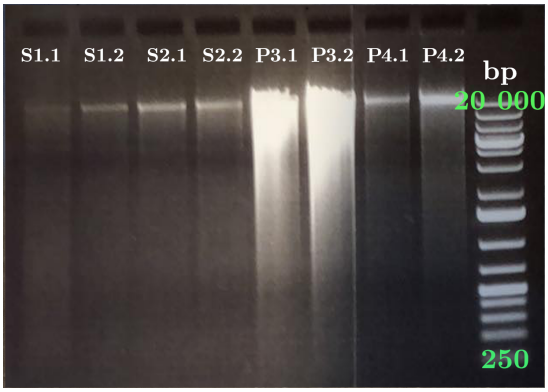

***Figure 4.11: Preliminary agarose gel electrophoresis of the CTAB-extracts**, to estimate fragment size. Ladder is the BenchTop 1kb Plus DNA ladder (250 - 20.000 bp). From left to right: S1.1-2, S2.1-2, **P**3.1-2, **P**4.1-2*

***Table 4.5: Enumeration of CFU's in the cultures of* C. Leadbeateri**. *When calculating Cells L^{-1}, the average CFU's in the controls were subtracted. The average CFU's from all 4 cultures are combined, and relative bacterial contamination found by dividing the upper and lower CI with their concurrent, estimated concentration of* C. Leadbeateri *at $t = 10.826$ (Table 4.3).*

Sample	C1	C2	S1	S2	S3	S4	Combined 99% CI	
							Upper	*Lower*
Count (10 FOV)	1	0	1	2	3	2	$\frac{1+2+3+2}{4} - \frac{1+0}{2} = \mathbf{2}$	
Cells L^{-1} ($C = 1.01e+06$)	1.01e+06	0.00e+00	5.03e+05	1.76e+06	1.88e+06	1.88e+05	1.03e+07	8.77e+04
				Estimated bacterial contamination at harvest (%)			7.16	0.06

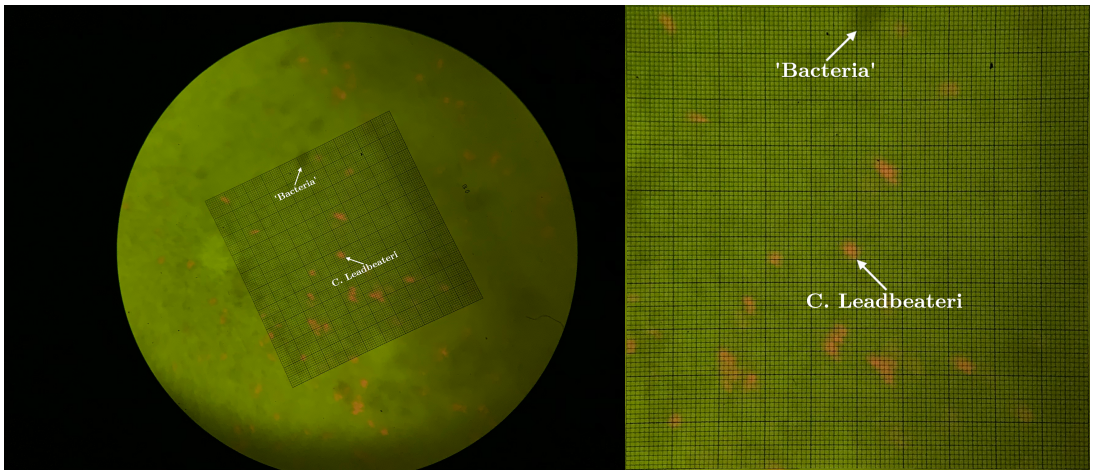

***Figure 4.12: Epifluorescence microscopy using DAPI stain** (400x magnification), of* C. leadbeateri *and CFU's of 'Bacteria'. The algae is seen as red dots, while a CFU were classified as a darker spot. The grid equals one 'field of vision' (FOV), measuring $0.5 \cdot 0.5 = 0.25\,mm^2$.*

4.4.2 Microbial gDNA-extraction from fish gills

Targeted gene sequencing of HAB-afflicted fish gill microbiome, affirming or denying the presence of *C. leadbeateri*, is beyond the intermediate scope of this thesis. In turn, the protocol developed to extract and amplify microbial gDNA from fish gills, has manifold uses - far beyond the application proposed in this study.

To help guide further work towards effective extraction of microbial gDNA from fish gills, we performed a series of quality control measures. DNA-yield, quality measurements and assessments for the different types of samples are showcased in Table 4.6 and Figure 4.14. Based on their 260:280 and -230 ratio, only 11 out of 63 samples were in the acceptable range for both measures. If we increased the upper and lower limit of this range by ± 0.05, an additional 11 samples would meet this criteria. Based on these measurements, we achieved the highest quality samples in those provided from the whole, frozen fish sourced in Tysfjorden.

Notated pictures of the amplified fish gill samples - from the gel electrophoresis and bioanalyzer - before and after subjecting our samples to the OneStep™ PCR Inhibitor Removal Kit, are shown under Figure 4.13. After the addition of removal kit, we could no longer see the 'smear' which we observed in the original, unadulterated samples.

We wondered if sample quality were reliant on the condition of the fish from which they were sampled from. In Table 4.7, the samples are grouped in the sample sets 'Live', 'Dead', or 'Whole'. Only a few of the sample sets were normally distributed and/or had equal variance, as such, the means and variances were mostly compared using non-parametric tests. In these, we found significant differences between the sample set 'Whole' and the other two groups.

The filtration time for the different samples varied widely. As such, we wondered if there was a correlation between filtration time and DNA-yield and -quality. Illustrated in Figure 4.15 are the different quality control measurements for the combined and singular sample types plotted against the filtration time. For the combined samples, a significant correlation was found between the filtration time and DNA yield. Though, this significance was not observed when rerunning the linear model for the singular sample sets.

Table 4.6: Showcasing the quality control measurements for the different sample types. *'In range' denotes how many of the samples that are in the acceptable range of both the 260:280 and -230 ratios - as described in section 3.5.1. ±0.05 Shows how many of the samples that are inside the acceptable range, if we increased their upper and lower limit by ±0.05. A = Astafjorden; G = Grøtsundet; K = Kattfjorden; T = Tysfjorden; Ss = Salmo salar; Cl = Cyclopterus lumpus; D = Dead; L = Live; W = Whole.*

	Sample type		All	A.*Ss*.D	G.*Ss*.W	K.*Cl*	K.*Ss*.D	K.*Ss*.L	T.*Ss*.D	T.*Ss*.L	T.*Ss*.W
		n =	63	4	6	4	6	8	9	9	17
A260:	A280	*Above*	40	4	5	4	5	7	6	5	4
		Below	0	0	0	0	0	0	0	0	0
	A230	*Above*	1	0	0	1	0	0	0	0	0
		Below	30	0	4	2	5	2	4	6	7
		In range	11	0	1	0	0	0	2	2	**6**
		±0.05	22	1	1	1	0	0	4	3	**12**
$ng \cdot \mu L^{-1}$	**[DNA]**	*Mean*	82.48	87.55	85.03	151.83	53.00	71.29	62.09	58.24	103.36
		SD	60.78	13.06	27.20	206.08	39.18	25.75	40.38	22.09	40.41

Table 4.7: Comparison of fish gill samples sampled from dead, live, and whole frozen fish *- in relation to the different quality control measurements. First rows shows values for the mean, variance (var.) and the Shapiro-Wilk test P-value (norm.) (Shapiro and Wilk, 1965). In the last rows, are the P-values from the comparison of the different sample sets.* ***Bold*** *values indicates where both sample sets follow a normal distribution, subjecting them to the F-test (Fisher, 1950). Otherwise, the variance of the samples sets have been compared using the non-parametric Fligner-Killen test (Fligner and Killeen, 1976). The means have been compared using the non-parametric Wilcoxon rank sum test, with continuity correction (Mann and Whitney, 1947). Significance codes: 0.05 '*'; 0.01 '**'; 0.001 '***'*

	260						**[DNA]**		
	280			230			$ng \cdot \mu L^{-1}$		
	Mean	*Var.*	*Norm.* (P)	*Mean*	*Var.*	*Norm.* (P)	*Mean*	*Var.*	*Norm.* (P)
Live	2.069	0.080^2	**0.426**	1.639	0.502^2	0.002**	62.61	24.53^2	0.831
Dead	2.089	0.154^2	3e-05***	1.738	0.392^2	0.202	81.90	91.13^2	9e-07***
Whole	1.978	0.047^2	**0.337**	1.697	0.404^2	0.002**	98.58	37.73^2	0.016*
P Live / Dead	0.786	0.569		0.673	0.797		0.664	0.033*	
P Live / Whole	3e-04***	**0.020***		0.948	0.418		0.002**	0.064	
P Dead / Whole	3e-05***	0.588		0.776	0.688		0.026*	0.588	

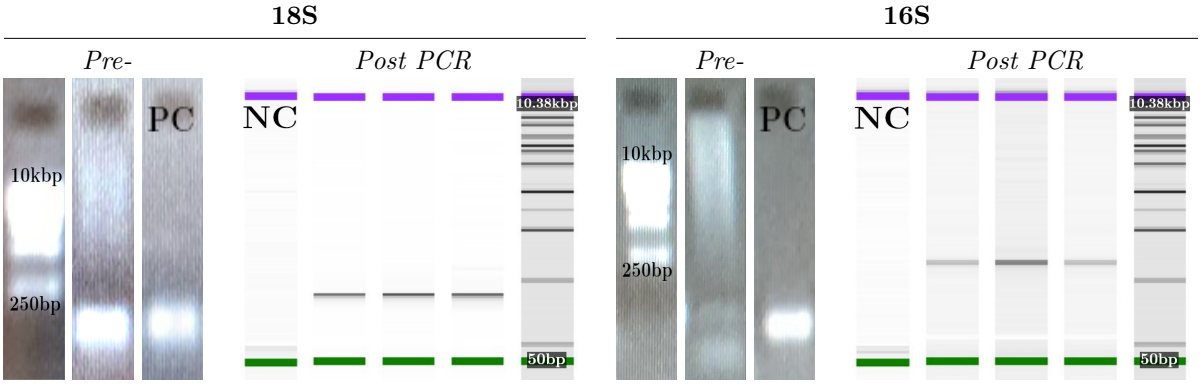

Figure 4.13: Amplified fish gill samples before (Pre-) and after (Post) the addition of the PCR-inhibitor removal kit *- as described in section 3.5.1. Samples in the agarose gel is paired with a BenchTop 1kb DNA ladder (250 - 10.000 bp). After the addition of removal kit, the bioanalyzer-results no longer fit the original description of 'smeared'. NC = Negative control; PC = Positive control; k = 1000; bp = base pairs.*

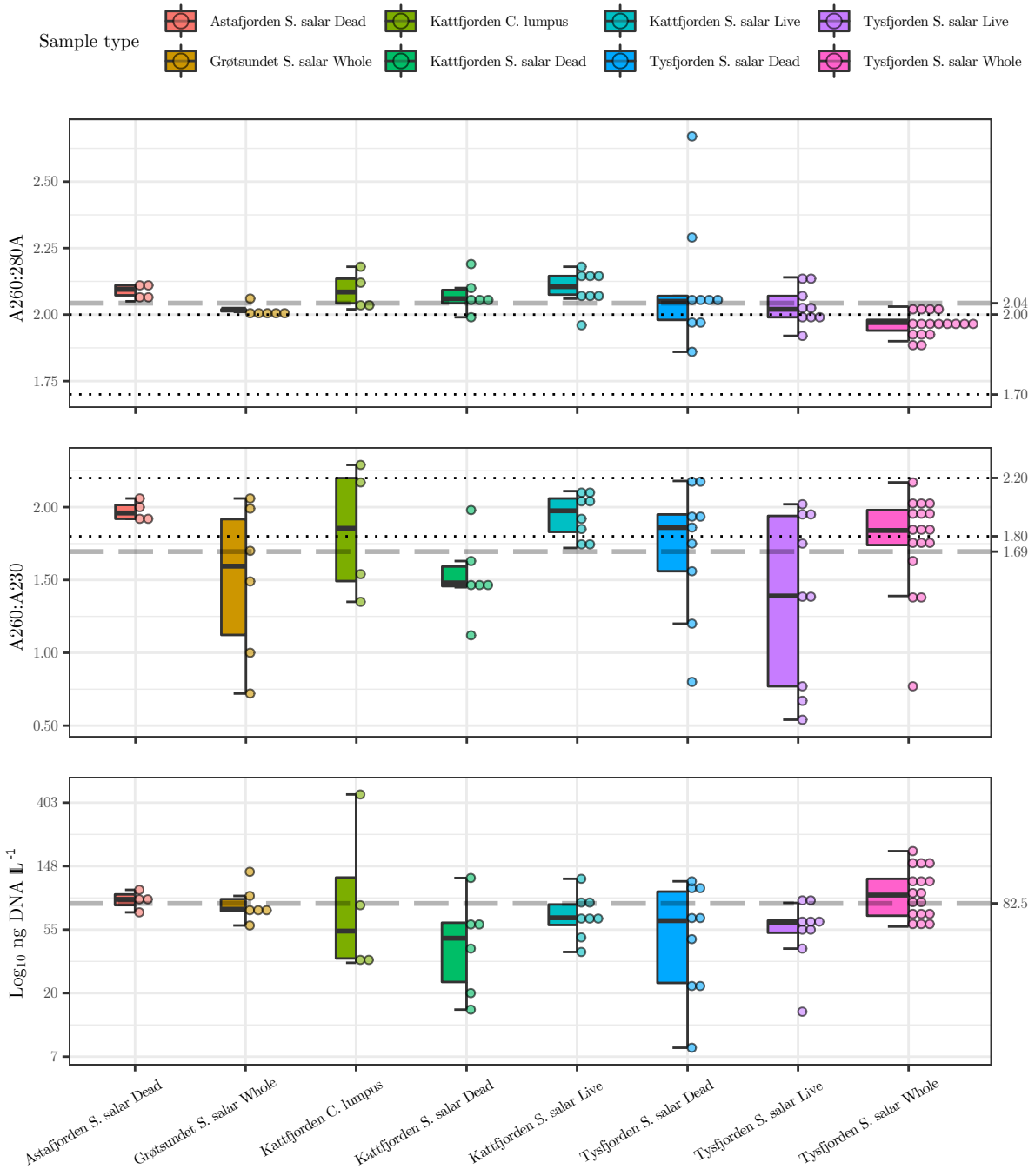

Figure 4.14: The quality control measurements for the different types of fish gill samples. *Black, dotted lines marks the upper and lower limit for the acceptable range of 280:260- and -230-ratios - as described in section 3.5.1. [DNA] is shown on log_{10}-scale. Gray, dashed lines is the mean for all the samples. For each sample type is shown a split box- and dotplot. Boxes shows interquartile length (IQR), the line indicates median, while whiskers are 1.5 IQR. The width of each box, is drawn proportional to the sample size. Dots indicate measurements for individual samples. Made using the 'ggplot' and 'gghalves' packages (Wickham, 2016; Tiedemann, 2020) in R.*

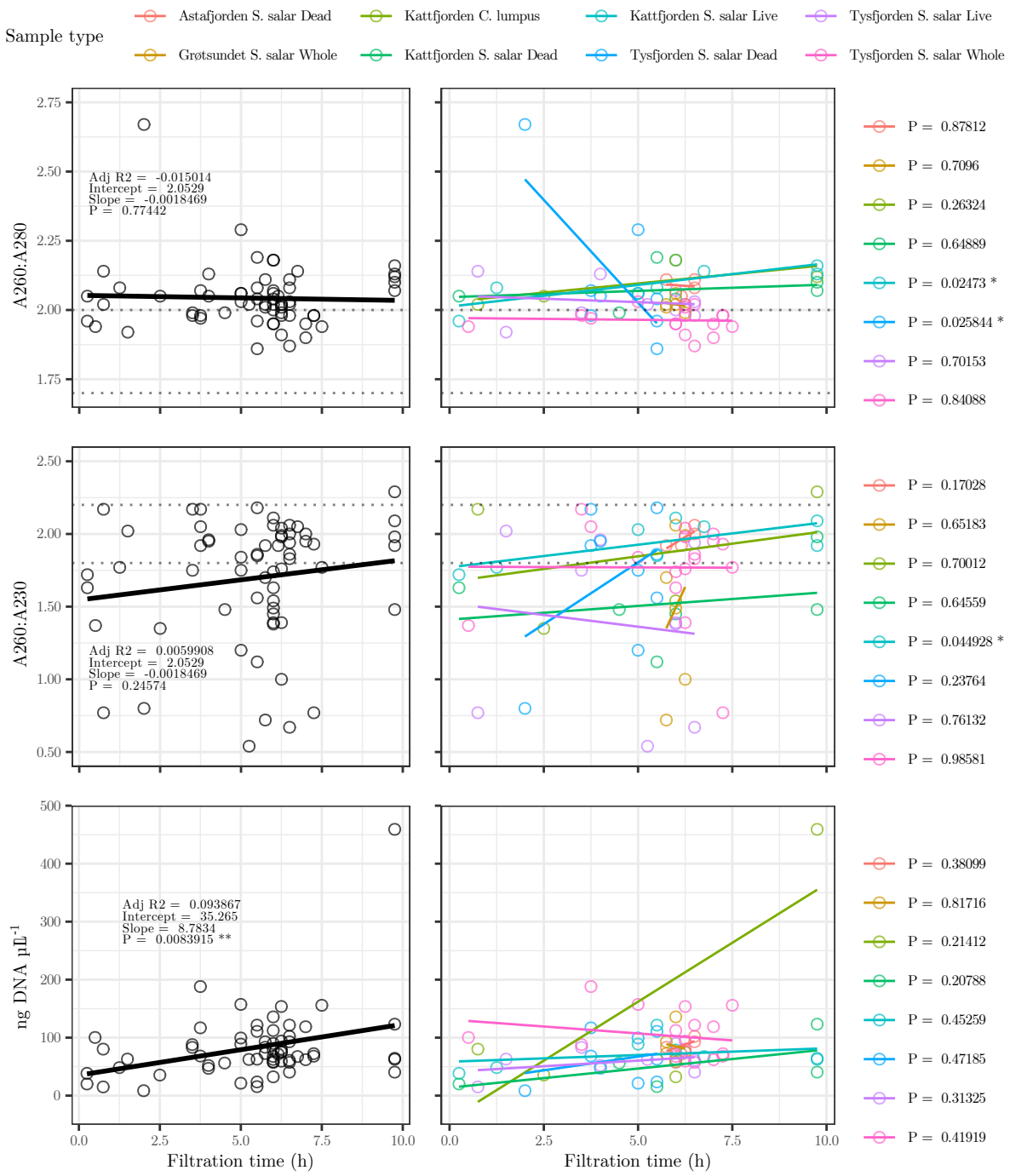

Figure 4.15: Linear regression model for the different quality control measurements, plotted against filtration time. *The Y-axis remains the same for vertically aligned plots. Likewise for horizontally aligned X-axis. Gray, dotted lines mark the upper and lower limit for the 280:260 and -230 ratio - as described in section 3.5.1. The leftmost plots, showcase the linear regression of the combined samples, also including relevant statistics from the lm()-function in R. Rightmost, is the plots for individual sample types, with the P-value from the linear regression model showcased in the immediate legend on the right. Significance codes: 0.05 '*'; 0.01 '**'. Made using the 'ggplot' and 'ggpubr' package (Wickham, 2016; Kassambra, 2020) in R.*

5 Discussion

5.1 Enumeration of *C. leadbeateri* in Troms

The original goal in analyzing the data collected by Akvaplan Niva, was to correlate *C. leadbeateri* cell counts with different environmental factors. Constrained by the data and expertise, this proved beyond the scope of this thesis. In addition to the data already presented, Akvaplan Niva also collected nutrient samples. These are yet to be processed.

The change in enumeration formats between May 23-27th and May 28-June 12th made it hard to make a continuous time-series for the whole period. Before May 28th, enumeration was performed in accordance with NS-EN 15204, while a simplified protocol was followed thereafter (section 3.1.3). The sampling before May 28th, was also performed at diversiform depths - afterwards, all enumeration samples were conjoined at 3 and 10 m. As such, the findings presented in this thesis, only pertains to the data collected after May 27th.

5.1.1 Fish mortality related to cell density of *C. leadbeateri*

Akvaplan Niva seemed to have constrained their sampling area to the northern part of Troms (Figure 3.3). Fortunately, only a few fish farms (Figure 2.3), North-West of Kvaløya, were afflicted. They also experienced a much lesser degree of mortality than the fish farms further south (Fiskeridirektoratet, 2019).

The mortality experienced at one of these fish farms, with concurrent *C. leadbeateri* cell counts is illustrated in Figure 4.1. *C. leadbeateri* cell counts peaked the day after they first experienced an anomalous increase in mortality. At the time, this fish farm had 4 pens with fish. It seems as if one of these pens experienced peak mortality a day before the others - while peak mortality in the other 3 pens corresponds to the peak in *C. leadbeateri* cell counts the day after.

A plausible scenario is rather that all 4 pens experienced peak mortality the same day. Hauling dead fish can be time consuming work, and if the shift end, so might the hauling - to be continued the next day. Even though the fish might have died the day before, the mortality date reported will, in most cases, be the day they hauled the fish. If this is true, Figure 4.1 might illustrate that peak mortality not necessarily corresponds with peak cell

counts of *C. leadbeateri*, but rather is a function of it's growth. If so, it might be possible that *C. leadbeateri* becomes toxic as a result of allelopathic interactions with other algae - producing toxins to inhibit the growth of their competitors.

5.1.2 Cell density of *C. leadbeateri*, and its relation to pycnocline strength and time

The highest density of *C. leadbeateri* were found in Balsfjorden, May 28th. Here, there where a marked difference between cell density at 3 and 10 m below the surface (Figure 4.3). We noticed a general trend in the data set; in the samples which were enumerated at both 3 and 10 m, *C. leadbeateri* cell density tended to be greater at 3 m.

As seen in Figure 4.4 a, there was indeed a higher density of *C. leadbeateri* cells at 3, compared with 10 m below the surface. Further, in Figure 4.4 b - from May 28th to June 12th - we see that when combining all locations, the mean concentration of *C. leadbeateri* cells was always greater at 3, compared with 10 m. This pattern would also be observed for singular locations (Figure 4.5), where the few antipodal observations (shown in gray) would also yield a much lesser disparity in cell counts (Figure 4.6). Figure 4.5 and 4.6 might also showcase that the disparity in cell density diminished in the latter part of the HAB, in concurrence with lower cell counts overall (Figure 4.4).

In the *C. leadbeateri* HAB of 1991, Rey et al. (1991) noted that there might have been an increased stratification of the water column. This might lead to non-uniform nutrient mixing, with a well-mixed surface layer on top of a poorly mixed deep layer (Mellard et al., 2011; Wetzel, 2001). Hence, we wondered if the observed cell density disparity might be a result of water stratification strength between 3 and 10 m.

Due to differing formats in the CTD-data collected, we chose to create a makeshift variable, indicative of the different stratifications: halocline (*salinity*), chemocline (*oxygenation*), termocline (*temperature*), and pycnocline (*density*). This was done by simply subtracting the CTD-values at 3 m and 10 m - supplying us with the variables which we correlated with cell density disparity in Table 4.1.

Seen in Table 4.1 - in a multiple regression containing all 4 stratifications measureable by the CTD - *oxygenation* proved of little value in the predictive model. Furthermore, out of all the predictive variables, *density* achieved the lowest P-value. *Density* is calculated as a

function of *salinity* and *temperature* (Jackett et al., 2006). As such, there would be a high degree of multicollinearity between the remaining variables (Mansfield and Helms, 1982).

Next, we created a multiple regression model containing *salinity* and *temperature*, and observed that, of the two, *salinity* had the lower P-value. In singular regression models for the three variables, *density* (labelled >06-13 in Table 4.1) achieved the lowest P-value. We continued the analysis only using this variable - labeling it 'pycnocline strength'.

As we assumed that the disparity between 3 and 10 m might have lessened in the latter parts of the sampling period (Figure 4.5), we wanted to see if this was reflected in a better fit for the linear regression model in certain time intervals. Shown in Table 4.1, are the temporally segregated regression models. The lowest P-value was observed in the times-series May 28th-June 5th - being two orders of magnitude greater than the other time-series examined.

It's important to note that, we've only checked the disparity in *C. leadbeateri* density between 3 and 10 m. From this, we can't extrapolate further, and for instance, claim that that, during the 2019 HAB, there was a higher density of *C. leadbeateri* cells closer to the surface. In a poorly mixed water column, the distribution of phytoplankton might vary tremendously (Mellard et al., 2011). Furthermore, during the latter stages of the *Prymnesium polylepis* HAB in Kattegat/Skagerrak of 1988, maximum cell concentrations were found within a thin layer at the pycnocline (Dahl et al., 1989). A similar pattern has been observed in unidentified haptophytes similar to *Chrysochromulina*- and *Prymnesium*-species in the Bay of Biscay (Farrell et al., 2014). Unfortunately, a deeper analysis of all the data collected, proved beyond the scope of this thesis.

5.2 Microbial gDNA-extraction

5.2.1 CTAB gDNA extraction from unialgal cultures

CCAP 1060, the Antarctic isolate of *P. glacialis* (Ø30-40 μm) (Thomas, 2005) is considerably larger than *C. leadbeateri* (Ø3-8 μm). Before subjecting *C. leadbeateri* to CTAB-gDNA extraction, we had routinely refined the protocol with cultures of *P. glacialis*, utilizing a 5 μm polycarbonate filters. Due to the size of *C. leadbeateri*, we deemed it necessary to utilize a smaller, 2.5 μm filter - made of paper, not polycarbonate.

When researching which filter type to use for harvest of *C. leadbeateri*, we were lead to believe that paper-based ones would be sufficient (Shi and Panthee, 2017). Of note, after suspending the filter paper in CTAB buffer for 1 hour, we saw little to no change in the colouration of the paper filters. Furthermore, the CTAB buffer had - in a much lesser degree than the polycarbonate *P. glacialis* samples - reached a satisfactorily level of 'muddiness'. We never harvested *C. leadbeateri* onto polycarbonate filters, and, as such, could not conclude if this was the causal factor behind the low DNA-yield (Table 4.4).

The hardships of isolating DNA from eukaryotic alga has repeatedly been reported (Healey et al., 2014; Jagielski et al., 2017). Commonly, this is thought to be caused by the constituents of their cell walls, which might include algenans, dinosporins, or silica compounds (Domozych et al., 2012; Siegel and Siegel, 1973). Haptophyte cells are commonly covered with tiny scales of organic material, mainly consisting of cellulose (1,4)-β-glucan) and acidic sheteroglykans, possibly with the addition of extracellular mucilages composed of complex heteroglykans (Myklestad and Granum, 2009).

In our *C. leadbeateri* samples, in general, there was a low A_{260}/A_{230}- and A_{260}/A_{230} ratio. One replicate of S1 was in the acceptable range for 'pure' DNA, while the others measured ± 0.05 outside of this range. The other replicate of S1 was the only sample which measured an 'acceptable' A_{260}/A_{230} ratio. This suggest that our samples contained some sort of contaminant - possibly due to some sort of carbohydrate carryover (Matlock, 2015).

When running the samples through agarose gel electrophoresis (Figure 4.11), we found that they all likely contained varying degrees of DNA product longer than >20 kb - besides sample P3, which we should have diluted further. Under conventional conditions, fragments which are larger than 20 kb co-migrate in a size-independent manner (Kaufmann, 1998). Instead of utilizing a static field, we should have rather utilized a pulsed-field gel electrophoresis (PFGE), to separate the different fragments (Schwartz and Cantor, 1984).

It's not uncommon to find cross-species contamination in genome sequencing projects (Merchant et al., 2014; Glassing et al., 2016). As we did not manage to achieve axenic cultures of *C. leadbeateri*, we found it prudent to estimate bacterial contamination in our samples. According to Muthukrishnan et al. (2017), counting bacteria using epifluorescence microscopy requires a minimum of 20 random fields of view (FOV), or a minimum of 350 bacterial cells to be a reliable measure of bacterial abundance. We only counted 10 FOV

for each sample. As all the samples had been treated the same, we also chose to combine them in the final enumeration.

The low bacterial abundance observed in our samples (Table 4.5) would, according to Chae et al. (2008), yield precise count data, but also a decline in accuracy. Hence the large confidence interval in the calculated bacterial abundance in our samples (Table 4.5). Commonly, the mean bacterial units found in each FOV is used to calculate bacterial abundance (Muthukrishnan et al., 2017). Due to the low level of bacteria in our samples, we instead treated bacterial contamination as a poisson variable - estimated using the same calculations used to determine cells/L in our Utermöhl counts (section 3.2.3).

5.2.2 gDNA-extraction from fish gills

Beyond either affirming or denying the presence of *C. leadbeateri* in afflicted fish gills, we also wished to study the kinship between our geographically distinct samples (Figure 3.1). The analysis also included samples from a locality which did not experience any HAB-related mortality in combination with rather high cell counts of *C. leadbeateri* (Figure 4.2). As such, we wondered if the presence of *C. leadbeateri* (and/or other microbes) 18S SSU rRNA in our fish gill samples, could be affiliated with HAB-related mortality.

The standard procedure for fish health personnel during an autopsy, is to store organs in a 10% neutral buffered formaldehyde-solution for histopathological examination (Veterinærinstituttet, 2020). This process reduces the molecular quality of nucleic acids (Feldman, 1973; Zimmermann et al., 2008), in most cases, making them unavailable for further amplification and analysis (Srinivasan et al., 2002; Douglas and Rogers, 1998). As freezing samples is not a consideration during a conventional fish health inspection, there was a severe lack of frozen samples from the earlier parts of the 2019 HAB.

Due to a global pandemic, we were not able to sequence our fish gill samples in time. We also utilized primers which were not optimized to amplify microeukaryotic DNA from vertebrate host tissue. To reduce the presence of host DNA, there exists host specific blocking primers (Vestheim and Jarman, 2008). This is also recommended by the Earth Microbiome Project in sequencing microeukaryotic 18S SSU rRNA - which encourages substituting the 1391F primer with the 'Mammal block I-short 1391f' mammal blocking primer, if there's a high probability of picking up host gDNA (Thompson et al., 2017).

Red blood cells (RBC) in fish - in contrast with mammals - is permanently nucleated (Glomski et al., 1992). Hence, we expected large amounts of fish gDNA to be amplified using the 18S SSU rRNA primers. When preparing our fish gill samples for harvest onto polycarbonate filtes, we utilized a 20 μm MESH (section 3.4). RBC's in *S. salar* are between 10.3-16.7 μm in diameter (Gulliver, 1875). Utilizing a smaller MESH size could possibly have removed some of the the RBC's. Though, as this was already a time consuming process (Figure 4.15), we chose not to.

In our quality control assessment, most of the fish gill samples had a low A_{260}/A_{230}-ratio, and a high A_{260}/A_{280}-ratio (Table 4.6). Going by Matlock (2015), the high A_{260}/A_{280} ratio is not indicative of an issue, while the low A_{260}/A_{230}-ratio is the result of a contaminant absorbing at 230 nm or less.

Going by the absorbance measurements (Table 4.6), the highest quality samples were achieved in the fish sampled in Tysfjorden. Especially the whole fish, which achieved the most acceptable absorbance profiles. This was not reflected in the whole fish samples from Grøtsundet, leading us to believe that the samples from Tysfjorden, in general, were of a higher quality than the rest of the samples. Incidentally, the only other whole fish samples were sourced from Grøtsundet, making it hard to compare the quality between different sample types (Whole, Dead, or Live).

When we did compare the A_{260}/A_{280}-ratio and DNA-concentration between the different sample types (Table 4.7), we found a statistical significant difference between the 'whole' and the other sample types. Though, as most of the 'whole' samples came from Tysfjorden, with few to compare from the other locations, this might not necessarily be related to the sample type. Though, looking at the three rightmost samples from Tysfjorden in Figure 4.14, we can see that the 'whole' samples have a more compact distribution, with more of the absorbance-measurements being in the 'acceptable range' (Table 4.6).

When the fish is of a smaller size, it's comparatively easier to freeze down whole fish, rather than sampling the gills on-site. For larger fish, cutting off the head, then freezing it, should yield a similar result. When receiving the whole frozen fish, we can also make sure that the gill extraction procedure is exact for all samples. As such, in hindsight, this would be the preferred sampling procedure for fish gills, if a HAB of similar characteristics were to happen again.

5.3 Growth characteristics for cultures of UIO-035

One of the original purposes and main goals of this experiment, was to compare the growth characteristics of UIO-035 with the isolates which we expected to cultivate. Unfortunately, we achieved no isolate cultures to compare with (section 4.3).

The experimental setup also failed to prove a linear correlation between Chl *a*-density and cell biomass and/or cell density. A common experimental setup is, in addition to measurements of Chl *a*, to make parallel measurements of carbon content per cell, resulting in the variable Chl:C - a key component in many microalgal growth models (Zonneveld, 1998; Bannister, 1979). In the original setup, this was deemed unnecessary, as our main goal was to establish a protocol from which we could compare UIO-035 with the growth characteristics of our isolates.

Microscope enumeration is a slow and tedious technique. In contrast, flow cytometry is much more rapid (Hofstraat et al., 1990; Stehouwer et al., 2013), expensive, and accurate - when enumerating cells in the 2-10 μm size range (Peperzak et al., 2020). If available, this would likely - for our use - be the superior method for cell enumeration.

Supplementary to the measurements presented in this paper, we also took daily images of each culture. In parallel with the Chl *a*-measurements, we transferred 4x2 mL sample from each culture onto a 4-well dish, photographing each well with a Zeiss AxioCam ERc 5s microscopy camera. Individual cells would be identified, and automatically counted, using the ImageJ software (Rasband et al., 1997). The cell density of the images would then be calibrated to the manual start- and end counts of each culture, giving us a decent proxy from which to correlate Chl *a* and cell density. Unfortunately, the software connected to our camera stopped working.

5.3.1 Growth characterization with no measurements in the stationary growth phase

To perform CTAB gDNA-extraction, we wanted to harvest our cultures in the exponential growth phase. As such, the growth experiment was cut short, with no measurements in the stationary phase. Hence, the projected growth curve presented in Figure 4.8, is only an extrapolation. As seen in Table 4.3, the projected carrying capacity (K) for the

cultures varied from 175.55 to 331.15 Chl *a* μg/L. Figure 4.8 might have looked different, if measurements continued into the stationary growth phase,

In addition to this, Figure 4.8 contains two Y-axis. It's important to note, that a change in measured Chl *a* μg/L dit not necessitate a similar change in cells/L. This relation was never proven in this experiment.

In calculating specific growth rates (μ), there were less variation (Table 4.3). If we were to achieve sustainable isolate culture from our water samples, this would be the main variable to compare between the different isolates. The experimental set-up could be repeated - attaining 5 measurements in the exponential growth phase (Table 4.2), before harvesting and possibly subjecting them to CTAB gDNA extraction.

5.3.2 Randomization of samples, or the lack there-of

Most phytoplankton species show diel variation in timing of cell division and the synthesis of various cell components (Chisholm and Costello, 1980; Wood et al., 2005; Manton and Parke, 1962). To account for this, we tried to perform measurements at the same time, each day, plus or minus one hour (Figure 4.8) - which might have proven unnecessary, as we conducted the experiment using a 24:0 continuous light cycle.

Rather, the order in which we measured our samples could have been randomized. As seen in the Chl *a*-based growth characteristics in Table 4.3, sample S4 have the highest standard error in the calculated growth rate (μSE). The replicates from this sample, was always the last to undergo *in vitro* Chl *a* measurements. As the whole procedure took between 1-2 hours to perform, the last samples to be examined might have been inordinately affected by temperature and light.

5.3.3 Settling time when performing manual Utermöhl counts

Utermöhl (1931) assumed that the day after preparing samples, all organisms would have settled and be ready for counting (Mazziotti et al., 2013). Later experience would revise this recommendation to 3 hours concerning samples of 2-3 mL, and 48 hours for 100 mL (Nauwerck, 1963; Hasle, 1978). We decided on a 24 hour settling time, due to the comparatively small size (Ø3-8 μm) of *C. leadbeateri* cells.

As shown in Table 4.3, at the *start* of cultivation, there is a gradual increase in cell counts from sample S4 to S1, which is also the order in which we counted the samples. Each sample consisted of 2 replicates, each of which were counted in 2 diagonally opposing transects. A single transect for each sample would be counted, before starting over, repeating the process for a total of 4 'rounds'. Each round took ∼1.5 hours to complete, possibly giving S4 an extra 1.5 hours of settling.

The gradual increase in counts were not observed for the samples at the *end* of cultivation. These were also counted in the opposite direction. Besides S4, S1-3 showed no significant difference in cell counts. In contrast with the other end count samples, the counts performed on S4 were significantly higher ($p < 0.001$, Table 4.3). Incidentally, there could have been more cells in this sample, though this was not reflected in the Chl *a*-measurements (Figure 4.7 and Table 4.2).

5.3.4 Variation in Utermöhl counts in relation to preservative used and preservation time

Variation in Utermöhl counts might be explained by the preservative used, in combination with preservation time. In experiments performed by Williams et al. (2016), there were substantial variation between the cell counts achieved using different dilutions and acidifications of Lugol's solution. Additionally, for all the different types of Lugol's solution, the cell counts varied, depending on how long the samples were preserved before counting. The variation they observed, also varied widely between different species[10].

The counts which we performed, at the *end* of cultivation, were diluted 1:14, and performed after 3 days of preservation at -4 ^{o}C. In contrast, the samples at the *start* of cultivation, were preserved for 15 days, before being counted. As such, the cell density variation observed between the samples from the *start* of cultivation, might have been due to increased cell degradation.

[10]Of note, when they counted the armoured dinoflagellate *Prorocentrum lima*, preservative used and preservation time had no significant effect on the measurements (Williams et al., 2016).

5.4 Isolation of *C. leadbeateri*-like Haptophyta

Though *C. leadbeateri* was reported as the focal strain and causal agent behind the 2019 HAB, this was based on taxonomic identification and assumptions made in 1991. As such, we wished to make isolates from the current bloom, not only to compare with UIO-035 - isolated in 1991 - but also between our isolates, from Kattfjorden and Grøtsundet.

C. leadbeateri has been found in a range stretching from the sub-Arctic to Antarctic (Eikrem et al., 2016). It displays a high degree of morphological variation, dependent on its origin (Eikrem et al., 2016). This would in a sense make it a 'cosmopolitan' species. de Vargas et al. (2007) proposes that such cosmopolitan species, could rather be sibling species, within a morphological superspecies (Eikrem et al., 2016).

Throughout the work on this thesis, some of our collaborators in the seafood industry asked if what was counted as *C. leadbeateri* in certain parts of Troms, might have been a different strain or species - morphologically similar, but non-toxic. In a similar vein, some also proposed that this was not a single bloom - inoculated from the epicenter of Ofot/Vestfjorden - but rather a series of blooms, originating in geographically distinct fjords, due to similar environmental and nutrient conditions. Some even considered heavy metal pollution from Russian nickel refineries (Bellona, 2020) - resident on the Kola Peninsula - as a potential catalyst for the HAB.

As such, the planned intra- (or maybe inter-) species comparison of our isolates - through growth rate characteristics, electron microscopy and, possibly, genomic sequencing - might have given strong credence, for or against, some of the hypothesises described above.

In a similar vein, we were also presented with the hypothesis that *C. leadbeateri* becomes toxic through allelopathic interactions with other algae - producing toxins to inhibit the growth of their competitors. While regularly observing our enriched samples, we did observe changes in the algal community over time. Unfortunately, when rechecking the cultures 198 days after their original enrichment (Figure 4.10), none had turned into unialgal cultures of *C. leadbeateri* through the allelopathic interactions we hypothesized.

5.4.1 Selenium - an essential trace mineral in the cultivation of *C. leadbeateri*?

We sourced our water samples from 3 different locations. When choosing which enrichment to source our isolates, we simply chose the ones with highest abundance of *C. leadbeateri*-like haptophyta. For 2 out of 3 samples (Figure 4.10) - both from Kattfjorden - this was from the cultures which had *not* been supplemented with selenium. Which might have been due to pure chance, as we did not supplement with selenium in most of our enrichments.

In an experiment by Edvardsen et al. (1990), the addition of 0.01 μM of selenite lead to a marked increase in *Prymnesium polylepis* cell density (previously known as *Chrysochromulina polylepis*). To our knowledge, a similar effect has not been documented in *C. leadbeateri*. Rhodes and Burke (1996), in their characterization of several non-*leadbeateri Chrysochromulina* isolates[11], found no significant increase in growth rate, when adding selenium to previously se-deprived cultures.

In cultures of *C. leadbeateri* UIO-035, Johnsen et al. (1999) added 20 nM selenium - which we also did, when measuring growth characteristics of the same strain (section 3.2.2). Likewise, when we enriched our water samples for isolation purposes, we added a selenium infused medium (TL-30) to 1 out of 4 samples, from each location. The culture collection from where we got the strain, also recommended the use of this medium (NORCCA, 2016). It contains 10 nM of selenium, of which we only supplemented half.

Selenium exists naturally in sea water (Ihnat, 1989), in concentrations of 1.14 (Schutz and Turekian, 1965) to 76 nM (Goldschmidt and Strock, 1935; Council et al., 1983). This is normally in the inorganic form of (+6) selenate and (+4) selenite (Martens, 2003). Organic forms of selenium are to be found in biologically active coastal areas (Wrench, 1983). As such, if selenium were to be an essential micronutrient for *C. leadbeateri*, supplementation might have been unnecessary - depending on where (Sugimura et al., 1976), and at what time (Wrench and Measures, 1982), we sourced our natural seawater.

[11] *C. acantha*, *C. ericina*, *C. hirta*, and *C. simplex*.

5.5 Mapping the 2019 HAB - spread and repercussions

At the time of writing this thesis, no reports comparable to the quality of Rey et al. (1991) have been published. As such, the general description of the 2019 HAB (section 2.2.2) was pieced together by cross-referencing the reports provided by Karlsen et al. (2019) and Marthinussen et al. (2020)[12], with the 'live' account given by Fiskeridirektoratet (2019). All this, combined with the mapping tools provided by ManolinAqua (2019) and BarentsWatch (2020), made it possible to sketch a rough timeline of the events, surrounding the 2019 HAB. Still - more than a year after the original event - we consider the available information, regarding its spread and biological repercussions, inadequate.

The description of events recited in the background (section 2.2.2) of this thesis, is by no means an official account of what actually happened, but a necessitated addition. The two reports currently published, was mainly focused on 'preparedness' (Karlsen et al., 2019) of the salmon farmers, or the economic consequences (Marthinussen et al., 2020) of the HAB. From the mortality figures we ourselves collected, we observed that the fish farm from which we sampled from in Tysfjorden (section 3.1.1.2) was afflicted at least twice - May 18th and 30th. Neither report records the date of these two events. Only May 30th is reported by Fiskeridirektoratet (2019).

Collecting mortality figures from all the afflicted fish farms, then using it to make a timeline - to some degree documenting the scope and progression of the HAB - was deemed beyond our capacity. In hindsight, it should not have been. A more detailed, 'mortality-based' timeline of events could have been an undemanding and fruitful addition to the thesis - at least in comparison with our arduous efforts in microbial genomics.

[12]Neither of these reports gave information about when, and how hard, singular localities were afflicted. Karlsen et al. (2019) produced a timeline, providing information on *when* and, to some degree, *how* different companies were afflicted, in addition to temporally unorganized, total mortality figures for individual fish farms. Marthinussen et al. (2020) included an anonymized map, of all the directly and indirectly HAB-afflicted localities - which we identified using BarentsWatch (2020).

6 Conclusion

- In water samples from Balsfjorden - May 28th - an estimated 48 607 600 cells/L of *C. leadbeateri* was found at 3 m below the surface.
- Increased fish mortality at a locality in Kattfjorden, temporally corresponded with a concurrent increase in *C. leadbeateri* cell density.
- In Northern Troms, during the 2019 HAB, there was a higher abundance of *C. leadbeateri* at 3 m, compared with 10 m below the surface.
- There is a chance that the observed difference in abundance of *C. leadbeateri* at 3 and 10 m could be attributed to the strength of the pycnocline - a relationship which might have peaked in the period May 28th-June 5th.
- When harvesting *C. leadbeateri*-like haptophyta for HMW CTAB gDNA extraction through filtration, it might be preferable to utilize a polycarbonate, rather than a paper filter.
- In our quality control assessments, filtration time had no measurable, adverse effect on the DNA yield and quality of our fish gill samples.
- When amplifying microbial gDNA from fish gills, it's preferable to use a host specific blocking primer.
- When collecting gill samples for microbial gDNA extraction, it's preferable to receive frozen whole fish and/or cut off fish heads.
- When using the Utermöhl manual counting technique on the *C. leadbeateri*-strain UIO-035, it's possible that settling time should exceed 3 hours.
- For performing Utermöhl counts on *C. leadbeateri*, Lugol's solution might not be an optimal preservative.
- When cultivating the *C. leadbeateri*-like haptophyta, it might not be necessary to supplement with selenium.

References

Allen, M., Poggiali, D., Whitaker, K., Marshall, T. R., and Kievit, R. A. (2019). Raincloud plots: a multi-platform tool for robust data visualization. *Wellcome open research*, 4.

Andersen, R. A. and Kawachi, M. (2005). Microalgae isolation techniques. *Algal culturing techniques*, pages 83–100.

Anderson, D. M. (2009). Approaches to monitoring, control and management of harmful algal blooms (habs). *Ocean & coastal management*, 52(7):342–347.

Anderson, D. M., Cembella, A. D., and Hallegraeff, G. M. (2012). Progress in understanding harmful algal blooms: paradigm shifts and new technologies for research, monitoring, and management. *Annual review of marine science*, 4:143–176.

Anderson, D. M., Stock, C. A., Keafer, B. A., Nelson, A. B., Thompson, B., McGillicuddy Jr, D. J., Keller, M., Matrai, P. A., and Martin, J. (2005). Alexandrium fundyense cyst dynamics in the gulf of maine. *Deep Sea Research Part II: Topical Studies in Oceanography*, 52(19-21):2522–2542.

Apprill, A., McNally, S., Parsons, R., and Weber, L. (2015). Minor revision to v4 region ssu rrna 806r gene primer greatly increases detection of sar11 bacterioplankton. *Aquatic Microbial Ecology*, 75(2):129–137.

Bannister, T. (1979). Quantitative description of steady state, nutrient-saturated algal growth, including adaptation. *Limnology and Oceanography*, 24(1):76–96.

BarentsWatch (2020). *Fiskehelse: Lakselus og fiskesykdommer i oppdrett*. https://www.barentswatch.no/fiskehelse [Accessed: 2020, March 12.].

Baumann, H. and Doherty, O. (2013). Decadal changes in the world's coastal latitudinal temperature gradients. *PloS one*, 8(6).

Bellona (2020). *Frykter mer forurensning i Nord-Norge*. https://bellona.no/nyheter/internasjonalt/russland/2011-10-frykter-mer-forurensning-i-nord-norge [Accessed: 2020, July 12.].

Berdalet, E., McManus, M., Ross, O., Burchard, H., Chavez, F., Jaffe, J., Jenkinson, I., Kudela, R., Lips, I., Lips, U., et al. (2014). Understanding harmful algae in stratified systems: Review of progress and future directions. *Deep Sea Research Part II: Topical Studies in Oceanography*, 101:4–20.

Berget, E. C. (2008a). *Denne krabaten herjer i Lofoten*. https://www.nrk.no/nordland/denne-krabaten-herjer-i-lofoten-1.5737340 [Accessed: 2020, April 9.].

Berget, E. C. (2008b). *Er på vei bort fra Lofoten*. https://www.nrk.no/nordland/er-pa-vei-bort-fra-lofoten-1.5761459 [Accessed: 2020, April 9.].

Berget, E. C. (2020). *Uttak av slaktet fisk fordelt på art 2005-2020 (Fylke)*. https://www.fiskeridir.no/Akvakultur/Tall-og-analyse/Biomassestatistikk/Biomassestatistikk-etter-fylke [Accessed: 2020, April 9.].

Black, E. (1990). Algal blooms in british columbia. *Harmful Algae Newsletter*, 3(2):11–12.

Bruno, D. W., Dear, G., and Seaton, D. D. (1989). Mortality associated with phytoplankton blooms among farmed atlantic salmon, salmo salar l., in scotland. *Aquaculture*, 78(3-4):217–222.

Bruslé, J. (1995). The impact of harmful algal blooms on finfish: mortality, pathology and toxicology. *IFREMER Reperes Ocean*, 10:1–75.

Brzezinski, M. A. (1985). The si: C: N ratio of marine diatoms: Interspecific variability and the effect of some environmental variables 1. *Journal of Phycology*, 21(3):347–357.

Burtis, C. A. and Bruns, D. E. (2014). *Tietz fundamentals of clinical chemistry and molecular diagnostics-e-book*. Elsevier Health Sciences.

Caporaso, J. G., Lauber, C. L., Walters, W. A., Berg-Lyons, D., Lozupone, C. A., Turnbaugh, P. J., Fierer, N., and Knight, R. (2011). Global patterns of 16s rrna diversity at a depth of millions of sequences per sample. *Proceedings of the national academy of sciences*, 108(Supplement 1):4516–4522.

CCAP (2009). *Strain Information: 1060/9*. https://www.ccap.ac.uk/strain_info.php?Strain_No=1060/9 [Accessed: 2020, July 21.].

Chae, G.-T., Stimson, J., Emelko, M. B., Blowes, D. W., Ptacek, C. J., and Mesquita, M. M. (2008). Statistical assessment of the accuracy and precision of bacteria-and virus-sized microsphere enumerations by epifluorescence microscopy. *Water research*, 42(6-7):1431–1440.

Chang, F. H., Anderson, C., and Boustead, N. C. (1990). First record of a heterosigma (raphidophyceae) bloom with associated mortality of cage-reared salmon in big glory bay, new zealand. *New Zealand journal of marine and freshwater research*, 24(4):461–469.

Chang, W. (2014). extrafont: Tools for using fonts. r package version 0.17.

Chisholm, S. W. and Costello, J. C. (1980). Influence of environmental factors and population composition on the timing of cell division in thalassiosira fluviatilis (bacillariophyceae) grown on light/dark cycles 1. *Journal of Phycology*, 16(3):375–383.

Chrétiennot-Dinet, M.-J., Desreumaux, N., and Vignes-Lebbe, R. (2014). An interactive key to the chrysochromulina species (haptophyta) described in the literature. *PhytoKeys*, (34):47.

Council, N. R. et al. (1983). *Selenium in Nutrition: Revised Edition*. National Academies Press.

Dahl, E., Lindahl, O., Paasche, E., and Throndsen, J. (1989). The chrysochromulina polylepis bloom in scandinavian waters during spring 1988. In *Novel phytoplankton blooms*, pages 383–405. Springer.

Dahl, E. and Tangen, K. (1993). 25 years experience with gyrodinium aureolum in norwegian waters. *DEV. MAR. BIOL. 1993*.

Dakshini, K. et al. (1994). Algal allelopathy. *The Botanical Review*, 60(2):182–196.

Davidson, K., Gowen, R. J., Harrison, P. J., Fleming, L. E., Hoagland, P., and Moschonas,

G. (2014). Anthropogenic nutrients and harmful algae in coastal waters. *Journal of environmental management*, 146:206–216.

de Vargas, C., Aubry, M.-P., Probert, I., and Young, J. (2007). Origin and evolution of coccolithophores: from coastal hunters to oceanic farmers. In *Evolution of primary producers in the sea*, pages 251–285. Elsevier.

Desjardins, P. and Conklin, D. (2010). Nanodrop microvolume quantitation of nucleic acids. *JoVE (Journal of Visualized Experiments)*, (45):e2565.

Díaz, P. A., Álvarez, A., Varela, D., Pérez-Santos, I., Díaz, M., Molinet, C., Seguel, M., Aguilera-Belmonte, A., Guzmán, L., Uribe, E., et al. (2019). Impacts of harmful algal blooms on the aquaculture industry: Chile as a case study. *Perspect. Phycol.*

Dommasnes, A., Rey, F., and Røttingen, I. (1994). Reduced oxygen concentrations in herring wintering areas. *ICES Journal of Marine Science*, 51(1):63–69.

Domozych, D., Ciancia, M., Fangel, J. U., Mikkelsen, M. D., Ulvskov, P., and Willats, W. G. (2012). The cell walls of green algae: a journey through evolution and diversity. *Frontiers in plant science*, 3:82.

Douglas, M. P. and Rogers, S. O. (1998). Dna damage caused by common cytological fixatives. *Mutation Research/Fundamental and Molecular Mechanisms of Mutagenesis*, 401(1-2):77–88.

Edvardsen, B., Eikrem, W., Throndsen, J., Saez, A. G., Probert, I., and Medlin, L. K. (2011). Ribosomal dna phylogenies and a morphological revision provide the basis for a revised taxonomy of the prymnesiales (haptophyta). *European journal of phycology*, 46(3):202–228.

Edvardsen, B. and Imai, I. (2006). The ecology of harmful flagellates within prymnesiophyceae and raphidophyceae. In *Ecology of Harmful Algae*, pages 67–79. Springer.

Edvardsen, B., Moy, F., and Paasche, E. (1990). Hemolytic activity in extracts of chrysochromulina polylepis grown at different levels of selenite and phosphate.

Eikrem, W., Medlin, L. K., Henderiks, J., Rokitta, S., Rost, B., Probert, I., Throndsen, J., and Edvardsen, B. (2016). Haptophyta. In *Handbook of the Protists*, pages 1–61. Springer.

Eikrem, W. and Throndsen, J. (1998). Morphology of chrysochromulina leadbeateri (prymnesiophyceae) from northern norway. *Phycologia*, 37(4):292–299.

Eilertsen, H. C. and Frantzen, S. (2007). Phytoplankton from two sub-arctic fjords in northern norway 2002–2004: I. seasonal variations in chlorophyll a and bloom dynamics. *Marine Biology Research*, 3(5):319–332.

Estep, K., Davis, P. G., Hargraves, P. E., and Sieburth, J. (1984). Chloroplast containing microflagellates in natural populations of north atlantic nanoplankton, their identification and distribution; including a description of five new species of chrysochromulina (prymnesiophyceae). *Protistologica (Paris. 1965)*, 20(4):613–634.

Farrell, H., Gentien, P., Fernand, L., Lazure, P., Lunven, M., Youenou, A., Reguera, B., and Raine, R. (2014). Vertical and horizontal controls of a haptophyte thin layer in

the bay of biscay, france. *Deep Sea Research Part II: Topical Studies in Oceanography*, 101:80–94.

Feldman, M. Y. (1973). Reactions of nucleic acids and nucleodroteins with formaldehyde. In *Progress in nucleic acid research and molecular biology*, volume 13, pages 1–49. Elsevier.

Finansdepartementet (2019). Skattlegging av havbruksvirksomhet. *Norges offentlige utredninger*, 2019(18).

Fisher, R. A. (1950). Contributions to mathematical statistics.

Fiskeridirektoratet (2019). *Algesituasjonen i nord*. https://www.fiskeridir.no/Akvakultur/Nyheter/2019/0519/Algesituasjonen-i-nord [Accessed: 2020, April 17.].

Fligner, M. A. and Killeen, T. J. (1976). Distribution-free two-sample tests for scale. *Journal of the American Statistical Association*, 71(353):210–213.

Forbes, S. H. (2020). pupillometryr: An r package for preparing and analysing pupillometry data. *Journal of Open Source Software*, 5(50):2285.

Fox, J., Weisberg, S., Adler, D., Bates, D., Baud-Bovy, G., Ellison, S., Firth, D., Friendly, M., Gorjanc, G., Graves, S., et al. (2020). car: Companion to applied regression. *R package version 3.0-8*.

Garces, E., Montresor, M., Lewis, J., Rengefors, K., and Anderson, D. M. (2010). Phytoplankton life cycles and their impacts on the ecology of harmful algal blooms. *Deep-sea research. Part 2. Topical studies in oceanography*, 57(3-4).

Gavis, J. et al. (1976). Munk and riley revisited: nutrient diffusion transport and rates of phytoplankton growth. *J. mar. Res*, 34(2):161–179.

Giner, G. and Smyth, G. K. statmod: Statistical modeling. *R package version 1.4.34*.

Glassing, A., Dowd, S. E., Galandiuk, S., Davis, B., and Chiodini, R. J. (2016). Inherent bacterial dna contamination of extraction and sequencing reagents may affect interpretation of microbiota in low bacterial biomass samples. *Gut pathogens*, 8(1):24.

Glomski, C. A., Tamburlin, J., and Chainani, M. (1992). The phylogenetic odyssey of the erythrocyte. iii. fish, the lower vertebrate experience. *Histology and histopathology*.

Gobler, C. J., Doherty, O. M., Hattenrath-Lehmann, T. K., Griffith, A. W., Kang, Y., and Litaker, R. W. (2017). Ocean warming since 1982 has expanded the niche of toxic algal blooms in the north atlantic and north pacific oceans. *Proceedings of the National Academy of Sciences*, 114(19):4975–4980.

Goldschmidt, V. and Strock, L. (1935). Zur geochemie des selens. ii, nachr. *Ges. Wiss. Göttingen, Math.-Phys. Kl. IV, NF*, 1:123–142.

Granéli, E. and Johansson, N. (2003). Effects of the toxic haptophyte prymnesium parvum on the survival and feeding of a ciliate: the influence of different nutrient conditions. *Marine Ecology Progress Series*, 254:49–56.

Granéli, E., Paasche, E., and Maestrini, S. Y. (1993). Three years after the chrysochromulina polylepis bloom in scandinavian waters in 1988: some conclusions

of recent research and monitoring. In *5th International Conference on Toxic Marine Phytoplankton, Newport, RI, October 28-November 1, 1991*, pages 23–32. Elsevier.

Grinde, L. and Mamen, J. (2019a). Klimatologisk månedsoversikt: April 2019. *Været i Norge*.

Grinde, L. and Mamen, J. (2019b). Klimatologisk månedsoversikt: Februar 2019. *Været i Norge*.

Grinde, L. and Mamen, J. (2019c). Klimatologisk månedsoversikt: Mai 2019. *Været i Norge*.

Grinde, L. and Mamen, J. (2019d). Klimatologisk månedsoversikt: Mars 2019. *Været i Norge*.

Guillard, R. and Hargraves, P. (1993). Stichochrysis immobilis is a diatom, not a chrysophyte. *Phycologia*, 32(3):234–236.

Guillard, R. R. (1975). Culture of phytoplankton for feeding marine invertebrates. In *Culture of marine invertebrate animals*, pages 29–60. Springer.

Guillard, R. R. and Ryther, J. H. (1962). Studies of marine planktonic diatoms: I. cyclotella nana hustedt, and detonula confervacea (cleve) gran. *Canadian journal of microbiology*, 8(2):229–239.

Gulliver, G. (1875). *Observations on the Sizes and Shapes of the Red Corpuscles of the Blood of Vertebrates...*

Guzmán, L., Campodónico, I., Antunovic, M., et al. (1975). Estudios sobre un florecimiento tóxico causado por gonyaulax catenella en magallanes. iv. distribución y niveles de toxicidad del veneno paralítico de los mariscos (noviembre de 1972-noviembre de 1973). In *Anales del Instituto de la Patagonia*.

Haigh, N. and Esenkulova, S. (2014). Economic losses to the british columbia salmon aquaculture industry due to harmful algal blooms, 2009-2012. *PICES Scientific Report*, (47):2.

Hallegraeff, G. M. (1983). Scale-bearing and loricate nanoplankton from the east australian current. *Botanica marina*, 26(11):493–516.

Hallegraeff, G. M. (1993). A review of harmful algal blooms and their apparent global increase. *Phycologia*, 32(2):79–99.

Hallegraeff, G. M. (2010). Ocean climate change, phytoplankton community responses, and harmful algal blooms: a formidable predictive challenge 1. *Journal of phycology*, 46(2):220–235.

Harrison, P., Yu, P., Thompson, P., Price, N., and Phillips, D. (1988). Survey of selenium requirements in marine phytoplankton. *Marine Ecology Progress Series*, pages 89–96.

Hasle, R. (1978). The inverted microscope method. *Phytoplankton manual*, pages 88–96.

Hattenrath, T. K., Anderson, D. M., and Gobler, C. J. (2010). The influence of anthropogenic nitrogen loading and meteorological conditions on the dynamics and toxicity of alexandrium fundyense blooms in a new york (usa) estuary. *Harmful Algae*, 9(4):402–412.

Havforskningsinstituttet (2019a). *Dette vet vi om den såkalte «dødsalgen» i Nord-Norge.* https://www.hi.no/hi/nyheter/2019/mai/dette-vet-vi-om-den-sakalte-dodsalgen-i-nord-norge [Accessed: 2020, April 17.].

Havforskningsinstituttet (2019b). *Tema: Norsk vårgytende sild.* https://www.hi.no/hi/temasider/arter/norsk-vargytende-sild [Accessed: 2020, April 14.].

Healey, A., Furtado, A., Cooper, T., and Henry, R. J. (2014). Protocol: a simple method for extracting next-generation sequencing quality genomic dna from recalcitrant plant species. *Plant methods*, 10(1):21.

Hegseth, E. N. and Eilertsen, H. C. (1991). Oppblomstringens forløp og årsaker. *Oppblomstringen av Chrysochromulina leadbeateri i Vestfjorden, mai-juni 1991: rapport fra et faglig arbeidsseminar.*

Heidal, K., Skreslet, S., Å., M., Eliassen, R., and og Frogh, M. (1991). Fordelingen av planktonalgen chrysochromulina leadbeateri og dens miljøbetingelser i vestfjorden 1991. *Oppblomstringen av Chrysochromulina leadbeateri i Vestfjorden, mai-juni 1991: rapport fra et faglig arbeidsseminar.*

HELCOM (2017). Monitoring of phytoplankton species composition, abundance and biomass.

Henry, L. and Wickham, H. (2020). Purrr: Functional programming tools. *R package version 0.3.4.*

Hersoug, B. (2014). Lakseoppdrett blir industri 1992-2002. In Hovland, E., Møller, D., Haaland, A., Kolle, N., Hersoug, B., and Nævdal, G., editors, *Norges fiskeri- og kysthistorie, bind 1: Over den leiken ville han rå*, chapter 8, pages 249–278. Fagbokforlaget, Bergen.

Hofstraat, J. W., Van Zeijl, W., Peeters, J., Peperzak, L., and Dubelaar, G. B. (1990). Flow cytometry and other optical methods for characterization and quantification of phytoplankton in seawater. In *Environment and Pollution Measurement Sensors and Systems*, volume 1269, pages 116–132. International Society for Optics and Photonics.

Holm-Hansen, O. and Riemann, B. (1978). Chlorophyll a determination: improvements in methodology. *Oikos*, pages 438–447.

Hoogenhout, H. and Amesz, J. (1965). Growth rates of photosynthetic microorganisms in laboratory cultures. *Archiv für Mikrobiologie*, 50(1):10–25.

Hope, R. M. (2013). Rmisc: Ryan miscellaneous. *R package version*, 1(5).

Horner, R. A., Garrison, D. L., and Plumley, F. G. (1997). Harmful algal blooms and red tide problems on the us west coast. *Limnology and Oceanography*, 42(5part2):1076–1088.

Hovland, E. (2014). Havbruksnæringen i krise 1989-1991. In Hovland, E., Møller, D., Haaland, A., Kolle, N., Hersoug, B., and Nævdal, G., editors, *Norges fiskeri- og kysthistorie, bind 1: Over den leiken ville han rå*, chapter 7, pages 215–248. Fagbokforlaget, Bergen.

Huse, G., Fernö, A., and Holst, J. C. (2010). Establishment of new wintering areas in herring co-occurs with peaks in the 'first time/repeat spawner'ratio. *Marine Ecology Progress Series*, 409:189–198.

Ihnat, M. (1989). *Occurrence and distribution of selenium*. CRC press.

Jackett, D. R., McDougall, T. J., Feistel, R., Wright, D. G., and Griffies, S. M. (2006). Algorithms for density, potential temperature, conservative temperature, and the freezing temperature of seawater. *Journal of Atmospheric and Oceanic Technology*, 23(12):1709–1728.

Jagielski, T., Gawor, J., Bakuła, Z., Zuchniewicz, K., Żak, I., and Gromadka, R. (2017). An optimized method for high quality dna extraction from microalga prototheca wickerhamii for genome sequencing. *Plant methods*, 13(1):77.

Jakobsen, R., Hansen, P. J., Daugbjerg, N., and Andersen, N. G. (2012). The fish-killing dictyochophyte pseudochattonella farcimen: adaptations leading to bloom formation during early spring in scandinavian waters. *Harmful algae*, 18:84–95.

Johannessen, T., Knutsen, J., and Paulsen, Ø. (1991). Effekter av chrysochromulina leadbeateri på oppdrettfisk og villfauna. *Oppblomstringen av Chrysochromulina leadbeateri i Vestfjorden, mai-juni 1991: rapport fra et faglig arbeidsseminar*.

Johnsen, G., Dalløkken, R., Eikrem, W., Legrand, C., Aure, J., and Skjoldal, H. R. (1999). Eco-physiology, bio-optics and toxicity of the ichthyotoxic chrysochromulina leadbeateri (prymnesiophyceae). *Journal of Phycology*, 35(6):1465–1476.

Johnsen, T. M., Eikrem, W., Olseng, C. D., Tollefsen, K. E., and Bjerknes, V. (2010). Prymnesium parvum: The norwegian experience 1. *JAWRA Journal of the American Water Resources Association*, 46(1):6–13.

Jones, H., Leadbeater, B., and Green, J. (1994). Mixotrophy in haptophytes. *SYSTEMATICS ASSOCIATION SPECIAL VOLUME*, 51:247–247.

Jourdain, E. and Vongraven, D. (2017). Humpback whale (megaptera novaeangliae) and killer whale (orcinus orca) feeding aggregations for foraging on herring (clupea harengus) in northern norway. *Mammalian Biology*, 86(1):27–32.

Kahle, D. and Wickham, H. (2013). ggmap: Spatial visualization with ggplot2. *The R journal*, 5(1):144–161.

Kamykowski, D. and Zentara, S.-J. (1977). The diurnal vertical migration of motile phytoplankton through temperature gradients 1. *Limnology and Oceanography*, 22(1):148–151.

Karlsen, K. M., Robertsen, R., and Hersoug, B. (2019). Kartlegging av hendelsesforløp og beredskap under giftalgeangrepet våren 2019-astafjorden, ofotfjorden, vestfjorden og tysfjorden. *Nofima AS*.

Kassambra, A. (2020). ggpubr: 'ggplot2' based publication ready plots. *R package version 0.3.0*, 3.

Kaufmann, M. E. (1998). Pulsed-field gel electrophoresis. In *Molecular Bacteriology*, pages 33–50. Springer.

Landstad, T. (2019). *Vannkraft, algekamp og laksedød i Vestfjordsystemet*. https://www.an.no/laks/vann/debatt/vannkraft-algekamp-og-laksedod-i-vestfjordsystemet/o/5-4-1026335 [Accessed: 2020, April 14.].

Lane, D. (1991). 16s/23s rrna sequencing. nucleic acid techniques in bacterial systematics (stackebrandt e & goodfellow m, eds).

Larsen, N., Moestrup, Ø., and Pedersen, P. (1994). Catalogue 1994. scandinavian culture centre for algae & protozoa. department of phycology. botanical institute. university of copenhagen.

Leadbeater, B. (1972). Identification, by means of electron microscopy, of flagellate nanoplankton from the coast of norway. *Sarsia*, 49(1):107–124.

Levitus, S., Antonov, J. I., Boyer, T. P., Locarnini, R. A., Garcia, H. E., and Mishonov, A. V. (2009). Global ocean heat content 1955–2008 in light of recently revealed instrumentation problems. *Geophysical Research Letters*, 36(7).

Lund, J., Kipling, C., and Le Cren, E. (1958). The inverted microscope method of estimating algal numbers and the statistical basis of estimations by counting. *Hydrobiologia*, 11(2):143–170.

Mackie, I., Pirie, L., Ritchie, A., and Yamanaka, H. (1997). The formation of non-volatile amines in relation to concentrations of free basic amino acids during postmortem storage of the muscle of scallop (pecten maximus), herring (clupea harengus) and mackerel (scomber scombrus). *Food Chemistry*, 60(3):291–295.

Mann, H. B. and Whitney, D. R. (1947). On a test of whether one of two random variables is stochastically larger than the other. *The annals of mathematical statistics*, pages 50–60.

ManolinAqua (2019). *Kart over algeoppblomstringen*. https://manolinaqua.com/algae.html [Accessed: 2019, December 9.].

Mansfield, E. R. and Helms, B. P. (1982). Detecting multicollinearity. *The American Statistician*, 36(3a):158–160.

Manton, I. and Parke, M. (1962). Preliminary observations on scales and their mode of origin in chrysochromulina polylepis sp. nov. *Journal of the Marine Biological Association of the United Kingdom*, 42(3):565–578.

Martens, D. (2003). Selenium. u: Ba stewart, ta howel (eds.), encyclopedia of water sciences.

Marthinussen, A., Nystøyl, R., Storhaug, H. R., Valle, P. S., and Gaarder, M. (2020). Økonomiske og samfunnsmessige konsekvenser av algeoppblomstringen i havbruksnæringen i nord-norge. *Kontali Analyse AS*.

Maso, M. and Garcés, E. (2006). Harmful microalgae blooms (hab); problematic and conditions that induce them. *Marine pollution bulletin*, 53(10-12):620–630.

Matlock, B. (2015). Assessment of nucleic acid purity. *Technical Note*, 52646.

Mazziotti, C., Fiocca, A., and Vadrucci, M. R. (2013). Phytoplankton in transitional waters: Sedimentation and counting methods. *Transitional Waters Bulletin*.

Medlin, L., Elwood, H. J., Stickel, S., and Sogin, M. L. (1988). The characterization of enzymatically amplified eukaryotic 16s-like rrna-coding regions. *Gene*, 71(2):491–499.

Medlin, L. K., Kooistra, W. H., Potter, D., Saunders, G. W., and Andersen, R. A. (1997). Phylogenetic relationships of the 'golden algae'(haptophytes, heterokont chromophytes) and their plastids. In *Origins of algae and their plastids*, pages 187–219. Springer.

Mellard, J. P., Yoshiyama, K., Litchman, E., and Klausmeier, C. A. (2011). The vertical distribution of phytoplankton in stratified water columns. *Journal of theoretical biology*, 269(1):16–30.

Merchant, S., Wood, D. E., and Salzberg, S. L. (2014). Unexpected cross-species contamination in genome sequencing projects. *PeerJ*, 2:e675.

Moestrup, O. (2009). Ioc-unesco taxonomic reference list of harmful micro algae. *http://www. marinespecies. org/HAB*.

Montes, R. M., Rojas, X., Artacho, P., Tello, A., and Quiñones, R. A. (2018). Quantifying harmful algal bloom thresholds for farmed salmon in southern chile. *Harmful algae*, 77:55–65.

Moore, S. K., Trainer, V. L., Mantua, N. J., Parker, M. S., Laws, E. A., Backer, L. C., and Fleming, L. E. (2008). Impacts of climate variability and future climate change on harmful algal blooms and human health. In *Environmental Health*, volume 7, page S4. Springer.

Muthukrishnan, T., Govender, A., Dobretsov, S., and Abed, R. M. (2017). Evaluating the reliability of counting bacteria using epifluorescence microscopy. *Journal of Marine Science and Engineering*, 5(1):4.

Myklestad, S. M. and Granum, E. (2009). Biology of (1, 3)-β-glucans and related glucans in protozoans and chromistans. In *Chemistry, Biochemistry, and Biology of 1-3 Beta Glucans and Related Polysaccharides*, pages 353–385. Elsevier.

Nauwerck, A. (1963). *Die beziehungen zwischen zooplankton und phytoplankton im See Erken*. Lundequistska.

Neuwirth, E. (2014). Rcolorbrewer: Colorbrewer palettes. r package version 1.1-2. *The R Foundation*.

NORCCA (2016). *Chrysochromulina leadbeateri: UIO 035*. https://niva-cca.no/shop/coccolithophyceae-prymnesiophyceae/chrysochromulina/uio-035 [Accessed: 2020, June 5.].

NVE, N. v.-o. e. (2020). *NVE Atlas*. https://atlas.nve.no/Html5Viewer/index.html?viewer=nveatlas&layerTheme=null&scale=640000&basemap=&center=565174.8114654892%2C7589889.971576503&layers=0VyC4j0VyC4j3BHcOm [Accessed: 2020, April 17.].

Paerl, H. W. (1988). Nuisance phytoplankton blooms in coastal, estuarine, and inland waters 1. *Limnology and Oceanography*, 33(4part2):823–843.

Parada, A. E., Needham, D. M., and Fuhrman, J. A. (2016). Every base matters: assessing small subunit rrna primers for marine microbiomes with mock communities, time series and global field samples. *Environmental microbiology*, 18(5):1403–1414.

Pedersen, T. L. (2019). ggforce: Accelerating 'ggplot2'. *R package version 0.3.1*, 3.

Peperzak, L., Zetsche, E.-M., Gollasch, S., Artigas, L. F., Bonato, S., Creach, V., de Vré, P., Dubelaar, G. B., Henneghien, J., Hess-Erga, O.-K., et al. (2020). Comparing flow

cytometry and microscopy in the quantification of vital aquatic organisms in ballast water. *Journal of Marine Engineering & Technology*, 19(2):68–77.

Porter, K. G. and Feig, Y. S. (1980). The use of dapi for identifying and counting aquatic microflora 1. *Limnology and oceanography*, 25(5):943–948.

Puppo, C., Voisin, T., and Gontero, B. (2017). Genomic dna extraction from the pennate diatom asterionella formosa optimised for next generation sequencing.. *protocols.io*.

Raine, R., McDermott, G., Silke, J., Lyons, K., Nolan, G., and Cusack, C. (2010). A simple short range model for the prediction of harmful algal events in the bays of southwestern ireland. *Journal of Marine Systems*, 83(3-4):150–157.

Rasband, W. S. et al. (1997). Imagej.

Rensel, J. and Whyte, J. (2003). Finfish mariculture and harmful algal blooms. *Manual on harmful marine microalgae. Monographs on oceanographic methodology*, 11:693–722.

Rey, F. (1998). Toktrapport [3/6-8/6, 1998].

Rey, F. and Aure, J. (1991). Miljøforhold og mulige årsaker. *Oppblomstringen av Chrysochromulina leadbeateri i Vestfjorden, mai-juni 1991: rapport fra et faglig arbeidsseminar*.

Rey, F., Aure, J., Heidal, K., Skreslet, K., Mohus, Å., Eliassen, R., Frogh, M., Hegseth, E. N., Eilertsen, H. C., Throndsen, J., Eikrem, W., Johnsen, G., Johnsen, T. M., Lømsland, E. R., Meldahl, A.-S., Fonnum, F., Aune, T., Underdal, B., M., S. O., Johannessen, T., Knutsen, J. A., and Paulsen, Ø. (1991). Oppblomstringen av chrysochromulina leadbeateri i vestfjorden, mai-juni 1991: rapport fra et faglig arbeidsseminar.

Rhodes, L. and Burke, B. (1996). Morphology and growth characteristics of chrysochromulina species (haptophyceae= prymnesiophyceae) isolated from new zealand coastal waters. *New Zealand Journal of Marine and Freshwater Research*, 30(1):91–103.

Ricker, W. E. (1937). The concept of confidence or fiducial limits applied to the poisson frequency distribution. *Journal of the American Statistical Association*, 32(198):349–356.

Robson, J., Ortega, P., and Sutton, R. (2016). A reversal of climatic trends in the north atlantic since 2005. *Nature Geoscience*, 9(7):513–517.

Rockwood, L. L. (2015). *Introduction to population ecology*. John Wiley & Sons.

Schutz, D. F. and Turekian, K. K. (1965). The investigation of the geographical and vertical distribution of several trace elements in sea water using neutron activation analysis. *Geochimica et Cosmochimica Acta*, 29(4):259–313.

Schwartz, D. C. and Cantor, C. R. (1984). Separation of yeast chromosome-sized dnas by pulsed field gradient gel electrophoresis. *cell*, 37(1):67–75.

Shapiro, S. S. and Wilk, M. B. (1965). An analysis of variance test for normality (complete samples). *Biometrika*, 52(3/4):591–611.

Shi, R. and Panthee, D. R. (2017). A novel plant dna extraction method using filter paper-based 96-well spin plate. *Planta*, 246(3):579–584.

Shilo, M. (1967). Formation and mode of action of algal toxins. *Bacteriological Reviews*, 31(3):180.

Siegel, B. and Siegel, S. (1973). The chemical composition of algal cell walls. *CRC Critical Reviews in Microbiology*, 3(1):1–26.

Sopanen, S., Koski, M., Kuuppo, P., Uronen, P., Legrand, C., and Tamminen, T. (2006). Toxic haptophyte prymnesium parvum affects grazing, survival, egestion and egg production of the calanoid copepods eurytemora affinis and acartia bifilosa. *Marine Ecology Progress Series*, 327:223–232.

Sprouffske, K. and Wagner, A. (2016). Growthcurver: an r package for obtaining interpretable metrics from microbial growth curves. *BMC bioinformatics*, 17(1):172.

Srinivasan, M., Sedmak, D., and Jewell, S. (2002). Effect of fixatives and tissue processing on the content and integrity of nucleic acids. *The American journal of pathology*, 161(6):1961–1971.

SSB (1992). Fiske og oppdrett av laks mv. 1990. *Noregs offisielle statistikk*, NOS C(56).

Stehouwer, P. P., Liebich, V., and Peperzak, L. (2013). Flow cytometry, microscopy, and dna analysis as complementary phytoplankton screening methods in ballast water treatment studies. *Journal of applied phycology*, 25(4):1047–1053.

Stoeck, T., Bass, D., Nebel, M., Christen, R., Jones, M. D., BREINER, H.-W., and Richards, T. A. (2010). Multiple marker parallel tag environmental dna sequencing reveals a highly complex eukaryotic community in marine anoxic water. *Molecular ecology*, 19:21–31.

Sugimura, Y., Suzuki, Y., and Miyake, Y. (1976). The content of selenium and its chemical form in sea water. *Journal of Oceanography*, 32(5):235–241.

Šúri, M., Cebecauer, T., and Skoczek, A. (2011). Solargis: Solar data and online applications for pv planning and performance assessment. In *26th European photovoltaics solar energy conference*.

Tangen, K. and Dahl, E. (1993). Harmful phytoplankton in norwegian waters—an overview. In *Sixth International Conference on Toxic Marine Phytoplankton, Nantes, France*, page 195.

Thomas, D. P. (2005). Diatoms. In Scott, F. J. and Marchant, H. J., editors, *Antarctic Marine Protists*, chapter 2, page 84 and 86. Australian Biological Resources Study Canberra.

Thomas, M. K., Kremer, C. T., Klausmeier, C. A., and Litchman, E. (2012). A global pattern of thermal adaptation in marine phytoplankton. *Science*, 338(6110):1085–1088.

Thompson, L. R., Sanders, J. G., McDonald, D., Amir, A., Ladau, J., Locey, K. J., Prill, R. J., Tripathi, A., Gibbons, S. M., Ackermann, G., et al. (2017). A communal catalogue reveals earth's multiscale microbial diversity. *Nature*, 551(7681):457–463.

Throndsen, J. and Eikrem, W. (1991). Chrysochromulina leadbeateri og andre chrysochromulina arters biologi. *Oppblomstringen av Chrysochromulina leadbeateri i Vestfjorden, mai-juni 1991: rapport fra et faglig arbeidsseminar*.

Tiedemann, F. (2020). gghalves: Compose half-half plots using your favourite geoms. *R package version 0.1.0*, 1.

Treasurer, J. W., Hannah, F., and Cox, D. (2003). Impact of a phytoplankton bloom on mortalities and feeding response of farmed atlantic salmon, salmo salar, in west scotland. *Aquaculture*, 218(1-4):103–113.

Utermöhl, H. (1958). Zur vervollkommnung der quantitativen phytoplankton-methodik: mit 1 tabelle und 15 abbildungen im text und auf 1 tafel. *Internationale Vereinigung für theoretische und angewandte Limnologie: Mitteilungen*, 9(1):1–38.

Utermöhl, v. H. (1931). Neue wege in der quantitativen erfassung des plankton.(mit besonderer berücksichtigung des ultraplanktons.) mit 4 abbildungen im text. *Internationale Vereinigung für theoretische und angewandte Limnologie: Verhandlungen*, 5(2):567–596.

Vestheim, H. and Jarman, S. N. (2008). Blocking primers to enhance pcr amplification of rare sequences in mixed samples–a case study on prey dna in antarctic krill stomachs. *Frontiers in zoology*, 5(1):1–11.

Veterinærinstituttet (2019). Fiskehelserapporten 2018. *Veterinærinstituttets rapportserie*, 6(a).

Veterinærinstituttet (2020). Fiskehelserapporten 2019. *Veterinærinstituttets rapportserie*, 5(a).

Veterinærinstituttet (2020). *Prøvetaking av fisk: Prøver på formalin*. https://www.vetinst.no/provetaking-og-diagnostikk/hvordan-ta-ut-prover/provetaking-av-fisk [Accessed: 2020, June 9.].

Villain, A., Kojadinovic, M., Puppo, C., Prioretti, L., Hubert, P., Zhang, Y., Grégori, G., Roulet, A., Roques, C., Claverie, J.-M., et al. (2017). Complete mitochondrial genome sequence of the freshwater diatom asterionella formosa. *Mitochondrial DNA Part B*, 2(1):97–98.

Watson, Sue B.and Molot, L. (2013). Harmful algal blooms. In Férard, Jean-Françoisand Blaise, C., editor, *Encyclopedia of Aquatic Ecotoxicology*, pages 575–596. Springer Netherlands, Dordrecht.

Wehr, J. D. and Brown, L. M. (1985). Selenium requirement of a bloom-forming planktonic alga from softwater and acidified lakes. *Canadian Journal of Fisheries and Aquatic Sciences*, 42(11):1783–1788.

Wehr, J. D., Brown, L. M., and O'Grady, K. (1985). Physiological ecology of the bloom-forming alga chrysochromulina breviturrita (prymnesiophyceae) from lakes influenced by acid precipitation. *Canadian journal of botany*, 63(12):2231–2239.

Wetzel, R. G. (2001). *Limnology: lake and river ecosystems*. gulf professional publishing.

Wickham, H. reshape2: Flexibly reshape data: a reboot of the reshape package. *R package version 1.4.4*.

Wickham, H. (2016). *ggplot2: elegant graphics for data analysis*. Springer.

Wickham, H. (2019). stringr: Simple, consistent wrappers for common string operations. *R package version 1.4.0*.

Wickham, H., Francois, R., Henry, L., Müller, K., et al. (2020). dplyr: A grammar of data manipulation. *R package version 0.8.5*, 3.

Wickham, H. and Henry, L. (2020). tidyr: easily tidy data with "spread ()" and "gather ()" functions. r package version 1.1.0.

Wickham, H. and Seidel, D. (2020). scales: Scale functions for visualization. r package version 1.1.1.

Williams, O. J., Beckett, R. E., and Maxwell, D. L. (2016). Marine phytoplankton preservation with lugol's: a comparison of solutions. *Journal of Applied Phycology*, 28(3):1705–1712.

Wolfe, J. M. and Rice, E. L. (1979). Allelopathic interactions among algae. *Journal of Chemical Ecology*, 5(4):533–542.

Wood, A. M., Everroad, R., and Wingard, L. (2005). Measuring growth rates in microalgal cultures. *Algal culturing techniques*, 18:269–288.

Wrench, J. (1983). Organic selenium in seawater: levels, origins and chemical forms. *Marine Chemistry*, 12(2-3):237.

Wrench, J. and Measures, C. (1982). Temporal variations in dissolved selenium in a coastal ecosystem. *Nature*, 299(5882):431–433.

Wu, L., Cai, W., Zhang, L., Nakamura, H., Timmermann, A., Joyce, T., McPhaden, M. J., Alexander, M., Qiu, B., Visbeck, M., et al. (2012). Enhanced warming over the global subtropical western boundary currents. *Nature Climate Change*, 2(3):161–166.

Zimmermann, J., Hajibabaei, M., Blackburn, D. C., Hanken, J., Cantin, E., Posfai, J., and Evans, T. C. (2008). Dna damage in preserved specimens and tissue samples: a molecular assessment. *Frontiers in Zoology*, 5(1):18.

Zonneveld, C. (1998). A cell-based model for the chlorophyll a to carbon ratio in phytoplankton. *Ecological Modelling*, 113(1-3):55–70.

Appendix

A1 Algae-induced salmon mortality at (*redacted*) AS and (*redacted*) AS in Kaldfjorden May 1998

Akvaplan-niva
Fiolveien 15
9005 Tromsø
Telefon: 77 68 52 80
Telefax: 77 68 05 09

Rapporttittel /Report title
Algeindusert laksedød ved [redacted] AS og [redacted] AS i Kaldfjorden Mai 1998

Forfatter(e) / Author(s)	Akvaplan-niva rapport nr / report no:
Gjermund Bahr	APN412.98.1444
	Dato / Date: 09/06/98
	Antall sider / No. of pages 12
	Distribusjon / Distribution Begrenset/Restricted
Oppdragsgiver / Client [redacted] AS	Oppdragsg. ref. / Client ref. [redacted]

Sammendrag / Summary

Det konkluderes med at vannets fysiske kvalitet (oksygen, salt, temperatur) ikke har primær innvirkning på dødeligheten hos laksen i Kaldfjorden. Dødeligheten på laksen er trolig en effekt av oppblomstringen av *Chrysochromulina leadbeateri*. På grunn av den registrerte dødeligheten ved 1,5 mill. celler per liter sjøvann, er det viktig at algenes konsentrasjon kommer godt under dette før ny fisk settes ut.

Emneord:	Key words:
Chrysochromulina leadbeateri Dødlighet hos laks Kaldfjorden Troms	*Chrysochromulina leadbeateri* Mortality on salmon Kaldfjorden Troms

Prosjektleder / Project manager	Kvalitetskontroll / Quality control
Gjermund Bahr	Roger Velvin

© Akvaplan-niva

INNHOLDFORTEGNELSE

1. Sammendrag

Foreliggende rapport presenterer resultatene fra vannanalysene fra en undersøkelse Akvaplan-niva gjennomførte i Kaldfjorden den 27 - 28.05.98 for [redacted] AS. Undersøkelsen er utført ved oppdrettslokalitetene "Blåmannsvik" og "Henrikvik", samt på en lokalitet ved slakteriet i Kaldfjorden. Undersøkelsen omfattet vannprøvetaking for verdier analyser av antall arter/grupper og individer av fytoplankton per liter sjøvann, samt en test på algenes giftighet. I tillegg ble det utført hydrografiske registreringer mht. oksygen, saltinnhold, tetthet, temperatur i vannsøylen.

Undersøkelsen gav følgende resultater:

- Algen *Chrysocromulina leadbeateri* ble funnet med mellom 1,5 - 3,5 mill. celler per liter sjøvann.
- Algen viste en viss giftighet i laboratorieforsøk på *artemia*-nauplier.
- De hydrografiske registreringene har ikke påvist begrensende faktorer for fiskens overlevelse.

2. Innledning

2.1 Bakgrunn og formål

Akvaplan-niva AS ble engasjert av [redacted] AS v/ [redacted] til prøvetaking av vann i forbindelse med en akutt dødelighet på fisken i anlegget. Prøvetakingen besto i innsamling av vannprøver fra områdene i og ved tre lokaliteter i Kaldfjorden: "Henrikvik", "Blåmannsvik" og "slakteriet". Slakteriet er lokalisert i den indre del av Kaldfjorden hvor det også ble registrert dødelighet på laks i forbindelse med en brønnbåttransport. Laksen kom fra Hammerfest og hadde en normal oppførsel inntil den kom inn i Kaldfjorden. Til kai ved slakteriet ble det registrert høy og økende dødelighet på fisken. Brønnbåten hadde inntil da brukt fjordvannet til sirkulasjon i rommene. Den ytre vanntilførselen ble avstengt og vannet satt på resirkulering og oksygenering uten at positiv effekt ble registrert.

3. Materiale og metode

3.1 Områdebeskrivelse

Figur 1 Stasjonskart over Kaldfjorden. Plasseringen av stasjonene "slakteriet", "Henrikvik" og "Blåmannsvik" er ikke eksakt, men angir omtrentlig plassering i fjorden.

3.2 Hydrografi og vannprøver

Vannprøver ble hentet fra 1 og 3 meters dyp ved de aktuelle stasjonene (Figur 1). Til dette ble det benyttet en 2 liters vannhenter. Prøvene ble analysert for celletall av personell ved universitetet i Tromsø.

Målinger av temperatur, saltholdighet, tetthet og oksygen i en vertikalprofil fra overflate til bunn, ble utført med en SENSORDATA STDO-sonde. Måle-intervallet ble satt til 5 sekund, og instrumentet ble senket sakte nok til å oppnå minst en måling per meter gjennom hele vannprofilen. Dette ble utført på de tre aktuelle lokalitetene. Data ble lest ut og presentert som tolkbare plotter.

Artsbestemmelse av algen ble utført av universitetet i Oslo v/Eikrem. Det ble benyttet elektronmikroskopi i forbindelse med artsbestemmelsen.

Giftighetstest på *artemia* nauplier. Testen ble utført Artemiatesten står nærmere beskrevet i avsnitt 6.1.

Adresser og telefonnummer til personellet fra universitetet i Oslo er å finne i vedlegg 6.

4. Resultater og vurdering

Resultatene fra prøveinnsamlingen er presentert i Tabell 1 og Figur 2. Disse blir fortløpende kommentert i hvert avsnitt.

Siktedypet var ved prøvetakingen rundt 6 m, dette er et omtrentlig mål da det ikke ble benyttet sikteskive. Det var ikke grunnlag for å si at det var store tettheter av alger som eventuelt tettet fiskens gjeller. Fiskens oppførsel ble karakterisert som "svimete" før døden inntraff.

4.1 Vannprøver og hydrografi

Analysene av vannprøvene ble utført av personell fra universitetet i Oslo og Tromsø. Dataene ble videre bearbeidet av Akvaplan-niva AS.

4.1.1 Artsbestemmelse

Wenche Eikrem v/universitetet i Oslo gav følgende karakteristikk av vannprøvene fra Kaldfjorden: Få diatomeer og store dinoflagellater, variert nanoplankton(eks. flere krageflagellat arter, *Mamiella* sp., *Pyramimonas* sp., *Apedinella spinifera*, *Pseudopedinella* sp., nakne (små) dinoflagellater, *Paraphysomonas* sp.) med dominans av små (ca 5-10 mikrometer) *Chrysochromulina* arter som *C. leadbeateri*, *C. cf. minor* samt to ubeskrevne *Chrysochromulina* arter.

4.1.2 Celletall og grupper

Tabell 1 Celletall for vannprøver innsamlet i perioden 27-28 mai. Celletallet angir antall celler/alger per liter sjøvann. Chrysochromulina leadbeateri er merket i den røde kolonnen.

	DATO	HAPTO	OXYRRIS	CALLIACA	FLAG_IND	CYANOFLG	DINO	DIATOME	COCCOLIT
Blåmannsvik									
3m	27.05.88	1793163		176016	275025	55005	22002	11001	
1m	28.05.88	1536473	7334	297027	161348	11001	14668	7334	
3m	28.05.88	1628148		168682	234688	29336	3667	3667	
Henrikvik									
1m	28.05.88	1716156	14668	355699	249356	18335	25669		
3m	28.05.88	2112192	11001	418038	275025	88008			22002
Slakteriet									
1m	28.05.88	2328545	7334	289693	271358	14668	36670	11001	22002
3m	28.05.88	3542322		539049	616056	33003	11001	11001	

Arts - Acronymer:

HAPTO	= *Chrysocromulina leadbeateri*
OXYRRIS	= *Oxyrris* sp. (flagellat)
FLAG IND	= uidentifisert "liten" flagellat 3-6 mikrometer
DINO	= Dinoflagellater sp.
CALLIACA	= *Calliacantha* sp. (krageflagellat)
COCCOLIT	= *Coccolitophorida* sp. (kalkflagellat)
CYANOFLG	= *Cyanoflagellat* sp. (blågrønnalger)
DIATOME	= *Diatomea* sp.

Tettheten av *C. leadbeateri* varierte mellom 1,5 mill. (Blåmannsvik 3 m) og 3,5 mill. (Slakteriet 3 m) se Tabell 1 over.

4.1.3 Giftighetstest

Vannprøven fra 3 m (den 28. mai kl. 14.45) dyp ble inkubert i 24 timer ved 25°C. Av 125 testede dyr døde 3, dvs en dødelighet på 2.4%. I kontrollen med sjøvann døde ingen av de 60 testdyrene. Det var altså en antydning til forhøyet dødelighet i vannprøven i forhold til kontrollen, men denne kan ikke skilles fra gjennomsnittlig spontan dødelighet (0-2%) (Pers. med. Edvardsen).

4.1.4 Hydrografi

Det er kun registrert gode verdier på oksygenmetning i samtlige profiler. Metningen er på vel 100%. Saltinnhold er på mellom 30 og 34 promille. Temperaturen er registrert til mellom 6 og 3°C (Figur 2).

Det ikke registrert begrensende hydrografiske verdier. Verdiene for oksygen, temperatur og saltholdighet er tilstrekkelige for at laks skal kunne overleve.

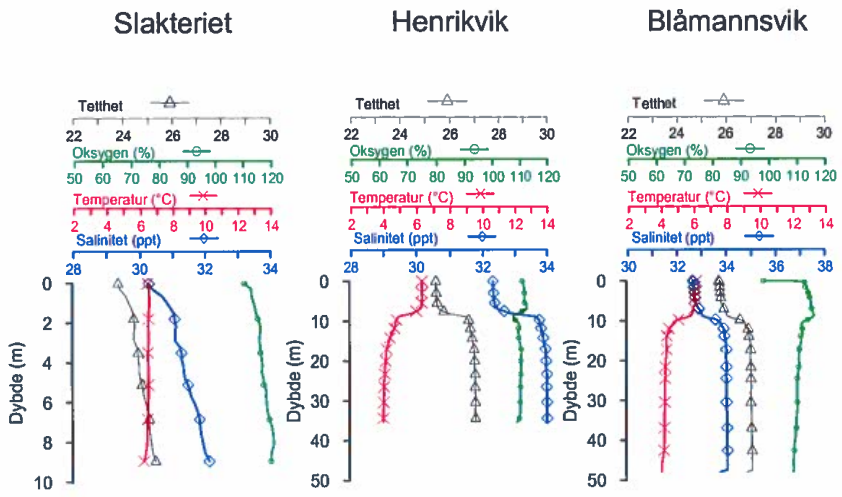

Figur 2 Hydrografi data innsamlet den 27.5.98 Fra lokalitetene: Slakteriet, innerst i Kaldfjorden; Henrikvik ca 3 km fra slakteriet og Blåmannsvik lengst ute i fjorden. Vær oppmerksom på skaleringen 10m - 50 og 50 m.

4.1.5 Sammenfattende vurdering

I 1991 ble det innrapportert dødelighet på fisk i Vestfjorden og Troms som en følge av forekomster av algen *Chrysokromulina leadbeateri* (Hegseth & Eilertsen 1991). Det er derfor nærliggende å tro at det er dette som er årsak til laksedøden i Kaldfjorden. *C. leadbeateri* viste lav dødelighet ved artemia - testing, men det er tidligere konkludert med at *C. leadbeateri* er en "vanskelig" alge. Den vil ofte endre karakter når man forsøker å jobbe med den i kultur i laboratoriet (pers. med. Eikrem). Artemiatesten gir derfor ikke noe eksakt bilde av giftigheten til algen.

Det konkluderes med at vannets fysiske kvalitet (oksygen, saltholdighet, temperatur) ikke har primær innvirkning på dødeligheten hos laksen i Kaldfjorden. Dødeligheten på laksen er trolig en effekt av oppblomstringen av *C. leadbeateri*. På grunn av den registrerte dødeligheten ved 1,5 mill. celler per liter sjøvann, er det viktig at algenes konsentrasjon kommer godt under dette før ny fisk settes ut.

5. Litteratur

Hegseth, E. N. & Eilertsen, H. C. Oppblomstringen av Chrysochromulina leadbeateri i Troms i mai/juni 1991. Oppblomstringens forløp og årsaker. Norges fiskerihøgskole, Universitetet i Tromsø, 9000 Tromsø.

6. Vedlegg

Bente Edvardsen
Section of Marine Botany, Department of Biology
University of Oslo, [redacted]
Phone: [redacted] Fax: [redacted]
E-mail: [redacted]

Wenche Eikrem
Section of Marine Botany, Department of Biology
University of Oslo, [redacted]
Phone: [redacted] Fax: [redacted]
E-mail: [redacted]

6.1 Giftighetstest med artemia-nauplier

ARC-test fra Artemia Reference Center, Ghent, Belgia

Metode beskrevet av P. Vanhaecke, G. Persoone, C. Claus, P Sorgeloos (1981). Ecotox. environ. Safety 5:382-387.
Metoden er brukt på algetoksiner bl.a. i: Edvardsen B. 1993. Toxicity of *Chrysochromulina* species (Prymnesiophyceae) to the brine shrimp, *Artemia salina*. In: *Toxic phytoplankton blooms in the sea* (Ed. by T.J. Smayda & Y. Shimizu), pp. 681-686. Elsevier, Amsterdam.

Materiale:

Cyster av *Artemia salina* (ca 100 mg)
SDS (layrylsulfat), stam-løsning 10% (10g/100mL)
Autoklavert 70% sjøvann, 1L
Separasjonskolbe 250 ml, 2 st
Akvariepumpe, silikonslanger, overganger, klemmer,
Autoklaverte tynne glassrør , 2 st
Celledyrkningsplater 4 st (Nunclon Multidish 24 wells, Roskilde, Denmark)
Automatpipetter med spisser (-1mL og -5mL)
Prøverør i glass, 21 st i stativ
Petriskåler (normal størrelse), 4 st.
Lupe
Vekstskap med temperaturen 25°C og lysstyrken ca. 100 µmol $m^{-2}s^{-1}$

Utførelse:

1) Cyster (ca 100 mg eller 1/10-1/5 rør) av *Artemia salina* tilsettes en separasjonskolbe med 250 ml 70% sjøvann, montert på stativ og med rikelig luftbobling (dag 1). Klekking foregår i vekstskap ved temperaturen 25°C og i kontinuerlig lys med lysstyrken ca. 100 µmol $m^{-2}s^{-1}$.

2) Etter ett døgn (dag 2) overføres de nyklekkede naupliene til pertiskåler og derifra med pipette til ny separasjonskolbe med ca. 100 mL sjøvann. Cyster som kommer med fjernes med pipette så godt det går. Napliene inkuberes ytterligere ett døgn ved de samme forholdene som ovenfor.

3) Etter ytterligere ett døgn (dag 3) er naupliene ferdigutviklede for bruk i giftighetsforsøk (naupliusstadie II eller III).

4) Til hvert kammer i celledyrkningsplatene overføres 10 nauplier med pipette. Minst mulig sjøvann overføres med disse. Tilsett nauplier til 20 kammer per vannprøve/kultur som skal testes (5 ulike konsentrasjoner og fire kammer for hver konsentrasjon) + 20 kammer for standard (SDS)+ 8 kammer for kontroller (sjøvann og ugiftig algekultur).

5) Nauplienes alder og tilstand kontrolleres under lupe. Nauplier som ikke svømmer eller nauplier i stadium I erstattes med friske dyr. Cyster fjernes.

6) Cellekonsentrasjonen til algekulturenebestemmes med elektronisk partikkelteller (Coulter teller) (alt. manuelt med hemacytometer)

7) Fem ulike algekonsentrasjoner testes. Algekulturene fortynnes etter en log skala (f.eks. log10 eller log2). Hvis algenes giftighetsgrad er ukjent utføres først en "range-finding test". Algekulturene fortynnes da etter en log10-skala der den høyeste konsentrasjonen er den ufortynnede kulturen, dvs. 100%, 10%, 1%, 0,1% og 0,01% av algekulturen testes.

8) I vårt tilfelle er den omtrentlige giftighetsgraden kjent slik at vi direkte kan utføre en "Definitiv test" med konsentrasjoner fra en log2-skala som gir en mer nøyaktig verdi for LC50 (algekonsentrasjonen som gir 50% dødelighet). Den laveste algekonsentrasjonen som gav 100 % dødelighet i en "range-finding test" er her den høyeste konsentrasjonen som testes.

Vi skal fortynne våre kulturer slik at vi får konsentrasjonene 8000, 4000, 2000, 1000, 500 celler ml^{-1}. Pipetter 5 ml sjøvann (med temp. 17°C) i 4 rør og ha 10 ml kultur med 8000 celler ml^{-1} i ett rør. Merk rørene med algekonsentrasjonen. Fortynn algekulturene ved å ta 5 ml av den sterkere konsentrasjonen og tilsette et rør med 5 ml sjøvann osv. Bland ved å suge opp den fortynnede algeløsningen med automatpipetten og så tømme den ut, 2-3 ganger.

9) For å sjekke at nauplienes følsomhet er lik i hvert forsøk tilsettes en standardgift (SDS) til 20 kammer. Stamløsningen av SDS fortynnes x1000 med 70% autoklavert sjøvann (gir 0,01% eller 100 mg/L), denne fortynnede stamløsningen er holdbar i 48 timer. Følgende konsentrasjoner av SDS skal testes med tre replikater: 10, 13.5, 18, 32 mg/L. Dvs:

SDS mg/L	Volum SDS (0,01%) ml	Volum 70% sjøvann ml
10	1,0	9,0
13,5	1,35	8,65
18	1,8	8,2
24	2,4	7,6
32	3,2	6,8

LC50-24h-verdi for SDS bør ligge mellom 13.3 og 19.9 mg/L.

10) Som kontroll brukes 70% sjøvann i 4 replikater og en ufortynned kultur av en ugiftig helst nærbeslektet art (4 replikater).

11) Merk celledyrkningsplatene. 1 mL fra hvert rør tilsettes 4 ulike kammer (4 paralleller). Start med den laveste konsentrasjonen slik at samme pipettespiss kan brukes for hele fortynningserien.

12. Inkuber platene i ett døgn i vekstskap ved temperaturen 25°C og i mørker. Pakk platene inn i aluminiumsfolie.

13. Etter ett døgn (dag 4) telles levende og døde nauplier i hvert kammer under lupe. Dyr som ikke beveger seg i løpet av 10 sekunder regnes for døde.

14. Beregning av LC50-verdi: Algekonsentrasjonen logtransformeres. Prosent-andelen døde nauplier ved hver konsentrasjon probittransformeres (tabell). Plott probit-verdier som en funksjon av log-algekonsentrasjonen. Tilpass en rett linje enten på øyemål eller ved lineær regresjon (I dataprogrammet Cricket Graph velger du Curve fit, Simple). Les av fra kurven den algekonsentrasjon som gir probit-verdi 5 (= LC50 eller 50% dødelighet) eller sett in y=5 i uttrykket for regresjonslinjen og finn x. Det er kun resultatene fra den definitive testen som brukes ved beregninger av LC50-verdi.